Intramolecular Alkyl Phosphine Dehydrogenation in Cationic Rhodium Complexes of Tris(cyclopentylphosphine)

ARTICLE *in* CHEMISTRY · FEBRUARY 2008

Impact Factor: 5.73 · DOI: 10.1002/chem.200700954 · Source: PubMed

9 AUTHORS, INCLUDING:

Gabriele Kociok-Kohn
University of Bath
291 PUBLICATIONS **3,535** CITATIONS
SEE PROFILE

Stuart A Macgregor
Heriot-Watt University
134 PUBLICATIONS **3,613** CITATIONS
SEE PROFILE

Andrew Weller
University of Oxford
177 PUBLICATIONS **3,228** CITATIONS
SEE PROFILE

Prabha Vadivelu
National Institute for Interdisciplinary Scie…
14 PUBLICATIONS **210** CITATIONS
SEE PROFILE

CHEMISTRY
A EUROPEAN JOURNAL

DOI: 10.1002/chem.200700954

Intramolecular Alkyl Phosphine Dehydrogenation in Cationic Rhodium Complexes of Tris(cyclopentylphosphine)

Thomas M. Douglas,[a, b] Simon K. Brayshaw,[a] Romaeo Dallanegra,[a, b] Gabriele Kociok-Köhn,[a] Stuart A. Macgregor,*[c] Gemma L. Moxham,[a] Andrew S. Weller,*[a, b] Tebikie Wondimagegn,[c] and Prabha Vadivelu[c]

Abstract: $[Rh(nbd)(PCyp_3)_2][BAr^F{}_4]$ (**1**) [nbd = norbornadiene, Ar^F = $C_6H_3(CF_3)_2$, $PCyp_3$ = tris(cyclopentylphosphine)] spontaneously undergoes dehydrogenation of each $PCyp_3$ ligand in CH_2Cl_2 solution to form an equilibrium mixture of *cis*-$[Rh\{PCyp_2(\eta^2\text{-}C_5H_7)\}_2][BAr^F{}_4]$ (**2a**) and *trans*-$[Rh\{PCyp_2(\eta^2\text{-}C_5H_7)\}_2][BAr^F{}_4]$ (**2b**), which have hybrid phosphine–alkene ligands. In this reaction nbd acts as a sequential acceptor of hydrogen to eventually give norbornane. Complex **2b** is distorted in the solid-state away from square planar. DFT calculations have been used to rationalise this distortion. Addition of H_2 to **2a**/**b** hydrogenates the phosphine–alkene ligand and forms the bisdihydrogen/dihydride complex $[Rh(PCyp_3)_2(H)_2(\eta^2\text{-}H_2)_2][BAr^F{}_4]$ (**5**) which has been identified spectroscopically. Addition of the hydrogen acceptor *tert*-butylethene (tbe) to **5** eventually regenerates **2a**/**b**, passing through an intermediate which has undergone dehydrogenation of only one $PCyp_3$ ligand, which can be trapped by addition of MeCN to form *trans*-$[Rh\{PCyp_2(\eta^2\text{-}C_5H_7)\}(PCyp_3)(NCMe)][BAr^F{}_4]$ (**6**). Dehydrogenation of a $PCyp_3$ ligand also occurs on addition of $Na[BAr^F{}_4]$ to $[RhCl(nbd)(PCyp_3)]$ in presence of arene (benzene, fluorobenzene) to give $[Rh(\eta^6\text{-}C_6H_5X)\{PCyp_2(\eta^2\text{-}C_5H_7)\}][BAr^F{}_4]$ (**7**: X = F, **8**: X = H). The related complex $[Rh(nbd)\{PCyp_2(\eta^2\text{-}C_5H_7)\}][BAr^F{}_4]$ **9** is also reported. Rapid (≈5 minutes) *acceptorless* dehydrogenation occurs on treatment of $[RhCl(dppe)(PCyp_3)]$ with $Na[BAr^F{}_4]$ to give $[Rh(dppe)\{PCyp_2(\eta^2\text{-}C_5H_7)\}][BAr^F{}_4]$ (**10**), which reacts with H_2 to afford the dihydride/dihydrogen complex $[Rh(dppe)(PCyp_3)(H)_2(\eta^2\text{-}H_2)][BAr^F{}_4]$ (**11**). Competition experiments using the new mixed alkyl phosphine ligand $PCy_2(Cyp)$ show that $[RhCl(nbd)\{PCy_2(Cyp)\}]$ undergoes dehydrogenation exclusively at the cyclopentyl group to give $[Rh(\eta^6\text{-}C_6H_5X)\{PCy_2(\eta^2\text{-}C_5H_7)\}][BAr^F{}_4]$ (**17**: X = F, **18**: X = H). The underlying reasons behind this preference have been probed using DFT calculations. All the complexes have been characterised by multinuclear NMR spectroscopy, and for **2a**/**b**, **4**, **6**, **7**, **8**, **9** and **17** also by single crystal X-ray diffraction.

Keywords: C–H activation · hydrides · hydrogenation · phosphines · rhodium

Introduction

The activation and functionalisation of alkanes by transition metal complexes using homogeneous processes is an important area of research given the enormous synthetic value attached with changing C–H bonds into synthetically useful functional groups.[1–4] Alkane dehydrogenation by late transition-metal complexes represents one of the key areas of this effort as it allows alkanes to be converted into alkenes, an important chemical feedstock (Scheme 1).[5–8]

The majority of examples of alkane dehydrogenation require an acceptor (alkene) to, in effect, partake in a transfer

[a] T. M. Douglas, Dr. S. K. Brayshaw, R. Dallanegra, Dr. G. Kociok-Köhn, G. L. Moxham, Dr. A. S. Weller
Department of Chemistry, University of Bath
Bath BA27AY (UK)

[b] T. M. Douglas, R. Dallanegra, Dr. A. S. Weller
Department of Chemistry, Chemistry Research Laboratory
University of Oxford, Mansfield Road, Oxford OX13TA (UK)
Fax: (+44) 1865-272690
E-mail: andrew.weller@chem.ox.ac.uk

[c] Dr. S. A. Macgregor, Dr. T. Wondimagegn, Dr. P. Vadivelu
School of Engineering and Physical Sciences
William Perkin Building, Heriot-Watt University
Edinburgh, EH144AS (UK)
Fax: (+44) 131-451-3180
E-mail: s.a.macgregor@hw.ac.uk

Supporting information for this article is available on the WWW under http://www.chemeurj.org/ or from the author.

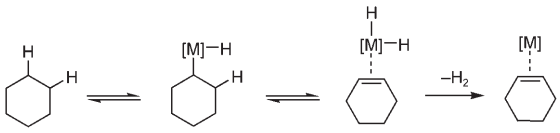

Scheme 1.

hydrogenation; although where a metal alkyl is present elimination of alkane can also act as a driving force for the reaction. Examples of intramolecular dehydrogenation from alkyl phosphines[9–12] (e.g. **I**,[13,14] **II**,[15,16] **III**[17,18]) and betadiketimates (**IV**[19–21]) are well-established; and other coordinated ligands, such as ethers,[22] alkoxides,[23] *N*-heterocyclic

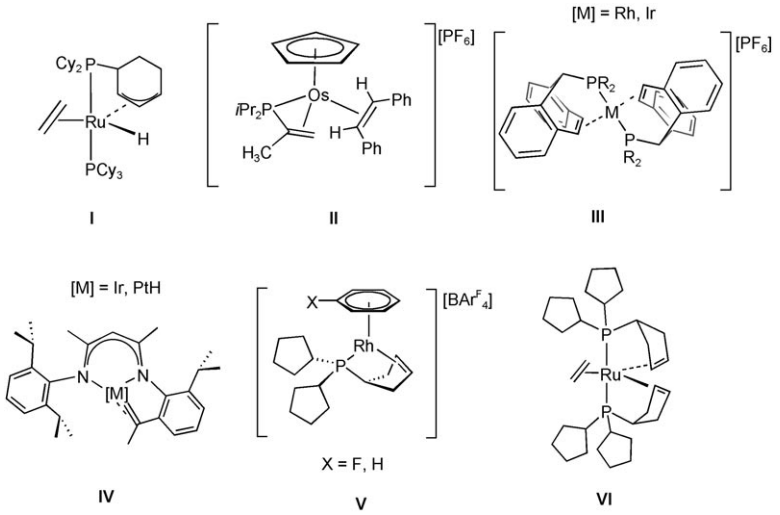

carbenes[24] and functionalised cyclopentadienyls[25] also undergo dehydrogenation. The intramolecular dehydrogenation of alkyl groups can also result in the addition of useful double-bond functionality that can be utilised for further elaborations in a synthetic scheme.[26,27]

One of our groups has recently communicated the intramolecular dehydrogenation of a cyclopentyl ring in tris(cyclopentylphosphine) ($PCyp_3$) to give **V**, by treatment of [Rh(nbd)Cl($PCyp_3$)] with Na[BAr^F_4] (as a halide abstracting reagent, nbd = norbornadiene, $Ar^F = C_6H_3(CF_3)_2$), with nbd acting as an acceptor of hydrogen from the cyclopentyl group.[28] When this reaction is performed in fluorobenzene or toluene the solvent coordinates (e.g., **V**), but when performed in weakly coordinating CH_2Cl_2 the [BAr^F_4]$^-$ anion complexes with the metal centre instead, through one of its arene rings.[29] Starting from [Rh(dppe)Cl($PCyp_3$)] this dehydrogenation reaction can be acceptorless, and also occurs at room temperature in less than five minutes.[28] Dehydrogenation of $PCyp_3$ on neutral ruthenium centres has also been very recently reported by Sabo-Etienne and Grellier by treatment of [$Ru(PCyp_3)_2(H)_2(\eta^2\text{-}H_2)_2$] with ethene.[30] This results in a double dehydrogenation to give **VI**, with the net loss of ten hydrogen atoms. Ours and Sabo-Etienne's observations clearly point to $PCyp_3$ being particularly well-set up for intramolecular alkyl phosphine dehydrogenation. Moreover, these transformations result in the concise generation of mixed phosphine/alkene ligands—a class of ligand that is currently attracting considerable interest in catalysis.[31,32] We report here, in full, our studies on the dehydrogenation chemistry of complexes containing one or two $PCyp_3$ ligands, including comparisons with tris(cyclohexylphosphine) ligands (PCy_3) and computational studies that shed light on mechanistic pathways, energies and the bonding in these complexes. As far as we are aware, prior to these recent studies, C–H activation in cyclopentylphosphine complexes has only been reported briefly before.[33,34] Of particular relevance to this paper are the extensive studies by Grützmacher on Group 9 metal complexes with chelating phosphine–alkene ligands derived from dibenzotropylidene phosphines such as diphenylphospanyldibenzocycloheptane ($tropp^{Ph}$) (e.g. **III**, see above, R = Ph).[17,18,35–41] Aspects of the work reported here have been communicated previously.[28]

Results and Discussion

Bis-$PCyp_3$ Complexes: The tris(cyclopentylphosphine) complex [Rh(nbd)($PCyp_3$)$_2$][BAr^F_4] (**1**) is prepared by addition of $PCyp_3$ to [Rh(nbd)Cl]$_2$ using Na[BAr^F_4] as a halide abstracting reagent in a biphasic CH_2Cl_2/H_2O solvent system. Although **1** can be isolated in analytically-pure form by low temperature recrystallisation, it is not stable in solution, unlike its tris(cyclohexylphosphine) (PCy_3) or tris(isopropylphosphine) ($PiPr_3$) analogues (which show no appreciable change in solution after 24 h in our hands). Over the course of 2 h in CH_2Cl_2 solution **1** smoothly converts to two new species, identified as a mixture of two isomeric complexes in which two cyclopentyl rings, one of each phosphine, have undergone alkyl dehydrogenation: *cis*-[Rh{$PCyp_2(\eta^2\text{-}C_5H_7)$}$_2$][$BAr^F_4$] (**2a**) and *trans*-[Rh{$PCyp_2(\eta^2\text{-}C_5H_7)$}$_2$][$BAr^F_4$] (**2b**) (Scheme 2). After 2 h the ratio of **2a**/**2b** is 3:1, respectively, but if left for 2 d (CD_2Cl_2 solution) this ratio changes to 1:3 after which there is no appreciable change. Heating to 40 °C overnight results in a change in ratio to 1:4, which on cooling eventually re-establishes the original concentrations. Thus, **2a** and **2b** are in equilibrium with one another, and although the barrier to rearrangement must be relatively high as it takes 2 d to approach equilibrium concentrations, there is only a small difference in relative stabilities ($K_{eq} \approx 3$; ΔG^0 (298 K) ≈ 2.5 kJ mol^{-1}). This high barrier reflects a possible reorgani-

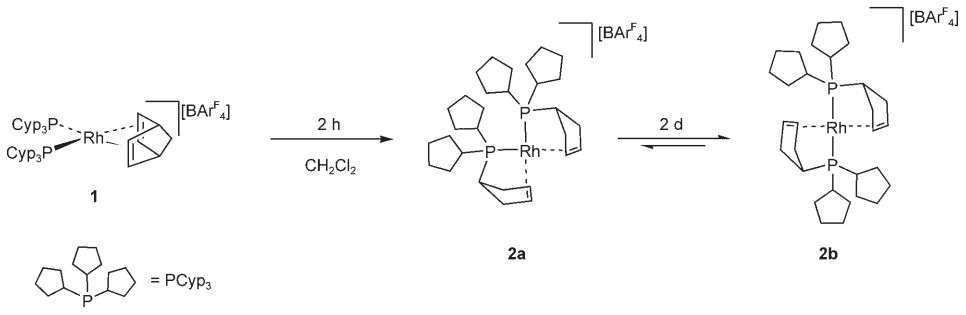

Scheme 2.

sation mechanism that involves partial decoordination of one of the strongly bound phosphine–alkene ligands or movement through a disfavoured rhodium(I) tetrahedral intermediate. A similar mixture of isomers, that do not interconvert on the NMR timescale, was observed for *cis*/*trans*-[Rh(tropp^{Ph})$_2$][PF$_6$].[38]

Complexes **2a** and **2b** have similar NMR spectroscopic characteristics, but subtle differences make the identification of the two isomers possible. In their ^{31}P{^{1}H} NMR spectra both display a single phosphorus environment showing coupling to ^{103}Rh [δ 67.4, J(Rh,P) = 150 Hz for **2a**; δ 65.8, J(Rh,P) = 114 Hz for **2b**]. The smaller RhP coupling constant for the *trans*-isomer **2b**, compared with the *cis*, is similar to the closely related complexes *cis*/*trans*-[Rh(tropp^{Ph})$_2$]-[PF$_6$],[38] and is an indication of the relative *trans* influences of the phosphine and alkene ligands. The ^{31}P chemical shift of the phosphines have undergone a significant downfield change, as expected for a ligand which has become part of a strained five membered ring.[42] For example, compared with cationic **1** [δ = 13.4] a chemical shift change of $\Delta\delta$ = +52.4 ppm occurs in **2b** on dehydrogenation and formation of the chelate ring. In the ^{1}H NMR spectrum distinctive resonances at δ = 4.90 (**2a**) and 5.46 ppm (**2b**) are observed for the chemically equivalent alkene protons in the dehydrogenated cyclopentyl rings on each isomer, with relative integrals of 1:3. No resonances at high field are observed, showing that there are no hydrides present. In the ^{13}C{^{1}H} NMR spectrum the alkene carbons for **2a** and **2b** are clearly identified at δ 100.0 and 89.2 ppm, respectively, both showing coupling to ^{103}Rh; with that for **2a** a AA′MM′X second-order system that shows *trans* coupling to ^{31}P. The relative downfield shift for the *trans* isomer is as noted for *cis*/*trans*-[Rh(tropp^{Ph})$_2$][PF$_6$].[38] The NMR spectra are unchanged on cooling to 250 K. Dissolving crystalline material of **2b** (see below) results in NMR spectra that show major peaks for the *trans* isomer, that slowly approach the equilibrium concentrations observed previously.

Compounds **2a** and **2b** are always formed as a mixture, and recrystallisation of the reaction mixture after 2 h affords crystals in which **2a** and **2b** have co-crystallised with both compounds in the unit cell. Leaving the reaction for 2 d, and then recrystallising, affords crystals of **2b** exclusively. Unfortunately the solid-state structures of the cocrystallised **2a** and **2b** result in a generally poor refinement from which we are reluctant to discuss the specifics of bond angles and distances. The gross structures of **2a**/**b** that derive from this analysis are presented in the Supporting Information, and confirm that they are *cis* and *trans* isomers, respectively. Grützmacher has reported the structure of *cis*-[Rh(^{Me}tropp^{Ph})$_2$][PF$_6$], which is closely related to **2a**.[37]

The solid-state structure of **2b**, crystallised from the solution left for two days, is presented in Figure 1. The phosphines are *trans* disposed [P-Rh-P 178.30(4)°], and although the Rh–P bond lengths [2.324(1), 2.327(1) Å] are a little longer than those reported for related bis(phosphine)–alkene complexes such as *cis*-[Rh(^{Me}tropp^{Ph})$_2$][PF$_6$][37] [average 2.241(1) Å] or [Rh(aminophosphole)(cod)][BF$_4$] [2.2116(7) Å],[41] they still are reasonable for a rhodium(I)–P bond. The Rh–C distances [ranging from 2.186(4)–2.192(4) Å] are also as expected for a rhodium(I)–alkene interaction, but are significantly shorter than found in *cis*-[Rh(^{Me}tropp^{Ph})$_2$][PF$_6$][35] [average 2.426(4) Å], which were noted for their unusual length. The C=C bond lengths [1.389(7), 1.388(6) Å] are as expected. The most notable feature of the molecule is that it is distorted so that the alkene units are compressed with regard to one another [∢ midpoint C3/C4–Rh–midpoint C23/C24 144.01(2)°] so that the carbon atoms C4 and C24 are almost linear [179.0(2)°], while the P-Rh-P angle is also essentially linear [178.30(4)°]. This distortion takes the molecule from idealised C_{2h} symmetry to approximate C_2 symmetry, and is reminiscent of that observed in the complex [Ru(CO)$_2$(P′Bu$_2$Me)$_2$].[43] The electronic reasons behind this distortion are discussed later and lie in the mutually *trans*, π-accepting alkene ligands. However, this distortion must also occupy a fairly shallow potential energy landscape as the solution NMR spectra of **2b** only shows one alkene environment (even at 250 K), whereas if the solid-state structure was retained there would be two, suggesting either a planar structure in solution or a low energy rocking occurs of the phosphine–alkene ligand. A related structure to **2b** has been reported for [Ir(tropp^{Ph})$_2$][PF$_6$], which shows a similar distortion although in this case is it defined as being more tetrahedral (P-Ir-P angles of 169.7°).[35] The newly formed phosphine-alkene ligand in **2a**/**b** has a bite angle (∢ P-Rh-centroid of C3/C4) of ≈83°, which is the same as that of dppe.

The formation of **2a**/**2b** comes as a result of a dehydrogenation of two cyclopentyl rings—one on each phosphine. Following the reaction by ^{1}H and ^{31}P{^{1}H} NMR spectroscopy allows intermediates on this process to be observed. Figure 2 shows a mole fraction/time plot for the organometallic complexes observed. Initially dissolving **1** in CH$_2$Cl$_2$ at 298 K affords a new complex, **3** (Scheme 3), very rapidly (minutes). After one hour the mole fraction of **3** starts to drop, eventually reaching zero, while those of **2a**, and then

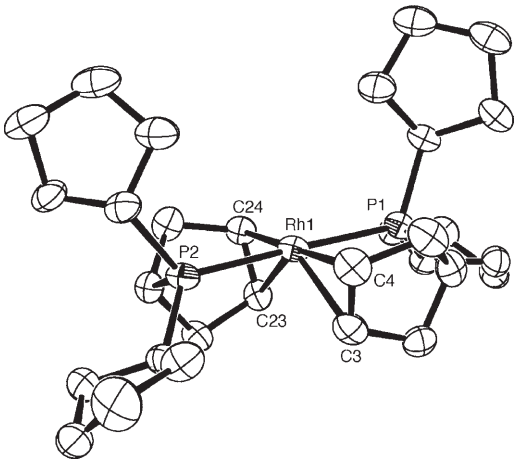

Figure 1. Solid-state structure of **2b**. Hydrogen atoms and the $[BAr^F_4]^-$ anion are not shown. Thermal ellipsoids are presented at the 50% probability level. Selected bond lengths [Å] and angles [°]: Rh1–P1 2.324(1), Rh1–P2 2.327(1), Rh1–C3 2.191(5), Rh1–C4 2.190(5), Rh1–C23 2.186(4), Rh1–C24 2.192(4), C3–C4 1.389(7), C23–C24 1.388(6), P1-Rh1-P2 178.30(4), P1-Rh1-Ct3/4 82.73(3), P2-Rh1-Ct23/24 82.66(3), Ct3/4-Rh1-Ct23/24 144.01(2), P1-Rh-Ct23/24 96.52(3), P2-Rh-Ct3/4 97.05(3).

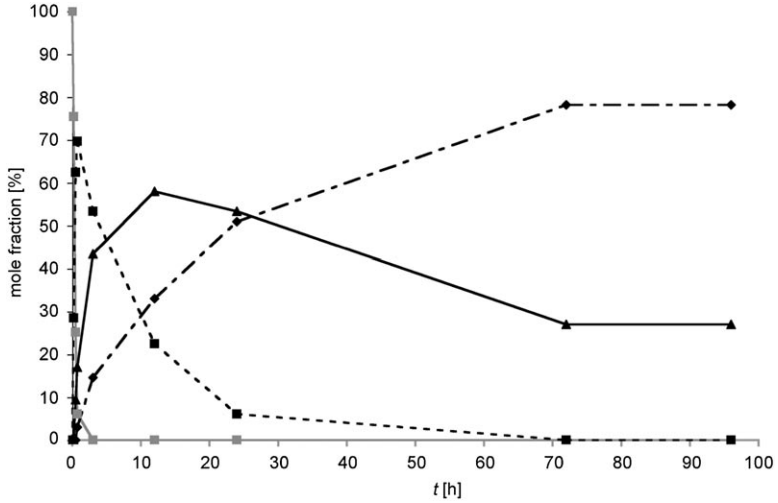

Figure 2. Plot of % composition of **1** (■), **2a** (▲), **2b** (◆) and **3** (■) for the reaction outlined in Scheme 2. Values from relative integrals in the ^{1}H NMR spectrum (normalised to 100%).

2b, rise. After 100 h there is no significant change in the composition of the solution. The mass balance remains constant, thus identifying **3** as an intermediate in the reaction. Compound **3** has been spectroscopically partially characterised as a norbornene (nbe) adduct *trans*-[Rh{$PCyp_2(\eta^2$-$C_5H_7)$}$(PCyp_3)(\eta^2$-nbe)][BAr^F_4] in which one of the cyclopentyl rings has undergone an alkyl dehydrogenation, with norbornadiene acting as a hydrogen acceptor to form norbornene. This activation process relies on dissociation of one of the $PCyp_3$ ligands, as in the presence of a 10-fold excess of $PCyp_3$ complex **1** remains unchanged in CH_2Cl_2 solution overnight. Complex **3** shows two broad resonances in the ^{31}P NMR spectrum [δ 75.7, 51.8] that, on cooling to 225 K, resolve into doublets-of-doublets that show coupling to ^{103}Rh and a large ^{31}P–^{31}P coupling [δ 76.2, J(P,P) = 286, J(Rh,P) = 120 Hz; δ 55.2, J(P,P) = 286, J(Rh,P) = 117 Hz], identifying a *trans* phosphine geometry. The hydride region of the ^{1}H NMR spectrum at this temperature is featureless. The data in hand do not allow us to conclusively state whether nbe is bound, or perhaps another weak interaction (agostic, solvent, adventitious water) is present, as, given the mixture, the ^{1}H NMR spectrum is ambiguous for identifying a coordinated nbe peak. In support of a nbe complex, **3** displays very similar ^{31}P{^{1}H} and ^{1}H NMR spectra to the well-characterised acetonitrile adduct *trans*-[Rh{$PCyp_2(\eta^2$-$C_5H_7)$}$(PCyp_3)$(NCMe)][BAr^F_4] (**6**) (see below) in which the phosphorus ligands lie *trans* both in solution and the solid-state. Whatever the nature of **3** it is clearly an intermediate on the overall double dehydrogenation process.

A suggested mechanism, based on that established for alkane dehydrogenation,[1,5,8] is presented in Scheme 3. Phosphine dissociation (**A**), C–H activation (**B**), β-H transfer (**C**) and then H_2 loss arrive at the intermediate species **3**. The transformation from **3** to **2a**/**2b** is much slower than that from **1** to **3** and presumably passes through a putative intermediate such as **D**. Although we have no direct evidence for a complex such as **D**, the isoelectronic complex *cis*-[Ru{$PCyp_2(\eta^2$-$C_5H_7)$}$_2H_2$] has been reported as an intermediate in the dehydrogenation of $PCyp_3$ in [Ru$(PCyp_3)_2(H_2)(\eta^2$-$H_2)_2$] using ethene as the acceptor to form complex **VI**.[30] We draw **D** as *cis* but it could well also be *trans*. Such isomerisation in dihydride phosphine complexes is known.[44] Given that we do not observe **D** in our system, and that **3** is relatively long-lived, the overall rate-determining step must be involved with the dehydrogenation of the second cyclopentylphosphine. Gas chromatographic analysis of the reaction mixture over the same timescale shows the nbd → nbe → nba conversion consistent with this strained alkene acting as a hydrogen acceptor. Although the mole fraction of nbd drops to zero, nbe is never completely converted into nba, suggesting that loss of H_2 from intermediate **D** is competitive with hydrogenation of nbe. Although **2a** and **2b** are in equilibrium with one another, given that they are both present in the reaction from the start we cannot discount a parallel mechanism that, in the early stages of the reaction, transforms **D** directly into **2b**.

We have been able to isolate a model for intermediate **D** in Scheme 3 by switching from rhodium to iridium. The related increase in M–H and M–P bond strength disfavours

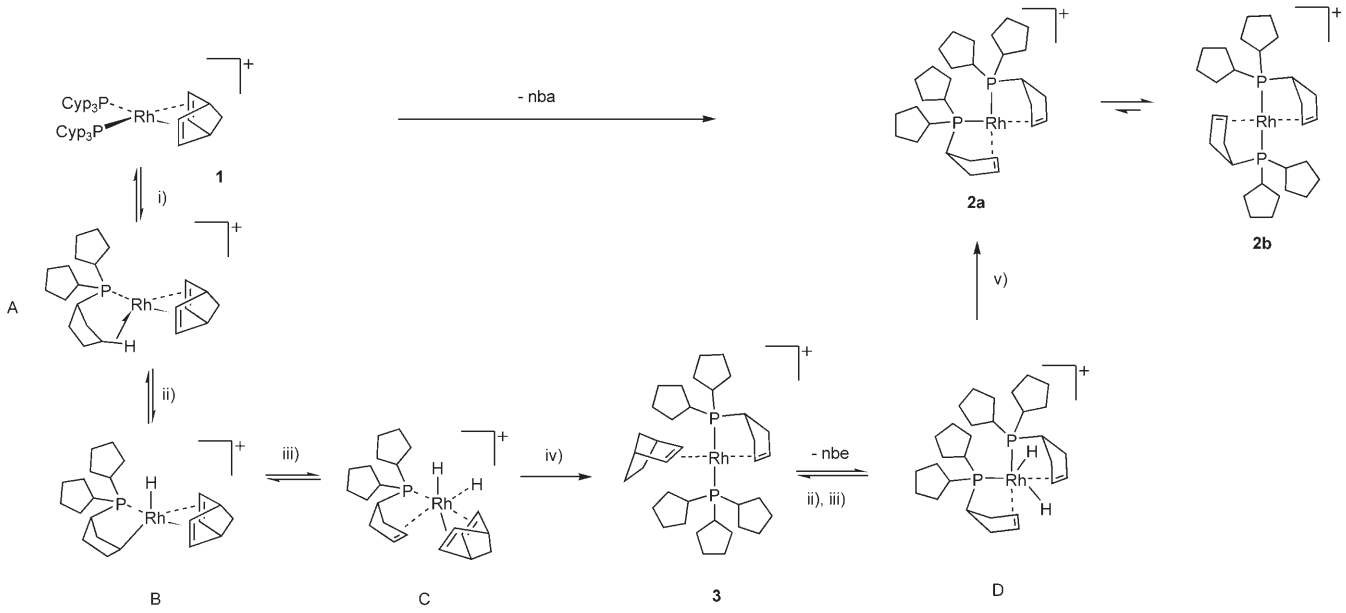

Scheme 3. Suggested mechanism for alkyl dehydrogenation in $PCyp_3$. i) $-PCyp_3$; ii) C–H activation; iii) β-H-transfer; iv) $+PCyp_3$ v) H_2 or nba.

hydrogen loss, either by elimination of H_2 or phosphine dissociation and reduction of nbe; allowing for the isolation of a complex in which both cyclopentyl groups have undergone dehydrogenation, but some of the hydrogen from this process remains on the metal. Addition of $PCyp_3$ to $[Ir(coe)_2Cl]_2$ along with $Na[BAr^F{}_4]$ and tbe (*tert*butylethene—an excellent hydrogen acceptor[5]) affords a complex mixture, as determined by ^1H and ^{31}P NMR spectroscopy, that after 16 h becomes one major species. This can be isolated as an analytically-pure crystalline material in moderate, 34%, yield and is identified by NMR spectroscopy and X-ray crystallography as *trans*-$[Ir(H_2)\{PCyp_2(\eta^2\text{-}C_5H_7)\}_2][BAr^F{}_4]$ (**4**). The solid-state structure of **4** shows a *trans* arrangement of phosphines with the alkene ligands mutually *cis* to one another and presumably *trans* to the hydrides, which were not located (Figure 3). A significant amount of disorder associated with the non-activated cyclopentyl groups could not be satisfactorily modelled due to the marginal quality of the data, meaning the hydride ligands on **4** were not located and it is inappropriate to discuss the structural metrics in detail. ^1H and $^{31}P\{^1H\}$ NMR spectroscopy show that a *trans* structure is retained in solution. In particular a single peak is observed in the $^{31}P\{^1H\}$ NMR spectrum at δ 39.5 ppm, while in the ^1H NMR spectrum a single resonance for chemically equivalent hydrides at δ −12.17 ppm is observed as a triplet [J(P,H) = 11.4 Hz], and the alkene protons are now observed as two, integral 2H, peaks at δ = 4.69 and 4.50 ppm. The related cation $[Ir(H)_2(tropp^{Ph})]^+$ (with various anions) forms on protonation of a neutral monohydride.[45] A solid-state structure has not been reported for this complex, but the NMR data compare well with **4**, in particular one ^{31}P environment and a triplet at δ −12.66 [J(P,H) = 11.8 Hz] for the two hydride ligands in the ^1H NMR spectrum.

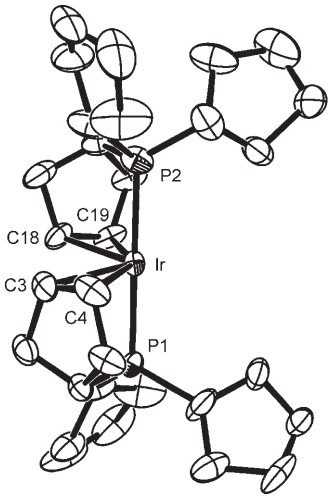

Figure 3. Solid-state structure of **4**. Hydrogen atoms and the $[BAr^F{}_4]^-$ anion are not shown. Thermal ellipsoids are presented at the 50% probability level. Selected bond lengths [Å] and angles [°]: Ir1–P1 2.308(2), Ir1–P2 2.326(2), P1-Ir-P2 179.5(1). The hydride ligands were not located. NMR data suggest that they occupy sites *trans* to the coordinated alkene ligands.

Addition of H_2 to the mixture of **2a**/**2b** results in the immediate hydrogenation of the bound alkene ligands and the generation, in quantitative yield by NMR spectroscopy, of the bisdihydrogen/dihydride complex $[Rh(PCyp_3)_2(H)_2(\eta^2\text{-}H_2)_2][BAr^F{}_4]$ (**5**) (Scheme 4). Complex **5** is directly analogous to $[Rh(PR_3)_2(H)_2(\eta^2\text{-}H_2)_2][BAr^F{}_4]$ (R = *i*Pr, Cy)[46] and the neutral ruthenium complexes $[Ru(L)_2(H_2)(\eta^2\text{-}H_2)_2]$ (L = PCy_3,[13] P*i*Pr$_3$,[47] $PCyp_3$,[48] *N*-heterocyclic carbene[49]). Complex **5** can be prepared more conveniently by direct addition of H_2 (4 atm) to **1**. Compound **5** is only stable under a H_2 atmosphere, decomposing to unidentified products when

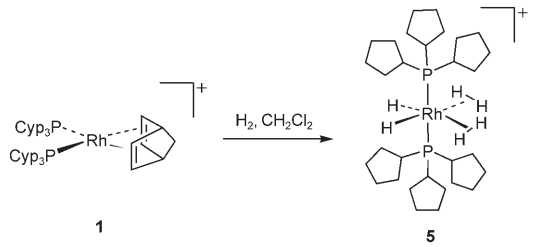

Scheme 4.

placed under a vacuum or the H_2 replaced with argon; the complex was fully characterised in solution by NMR spectroscopy. In the ^{1}H NMR spectrum at room temperature under a H_2 atmosphere no hydride signal is observed (presumably it is broad and unresolved in the baseline), and no signal for dissolved H_2 at δ 4.6 ppm is seen. This suggests rapid exchange between free and bound H_2, a common observation in dihydrogen systems at room temperature.[4] The ^{31}P{^{1}H} NMR spectrum shows a single phosphorus environment at δ 57.4 ppm [J(Rh,P) = 101 Hz]. Progressive cooling to 200 K results in two broad hydride signals at δ −2.21 and −13.79 ppm, in the ratio 4:2, respectively, with reference to the alkyl phosphine protons. T_1 relaxation time measurements at 200 K (400 MHz) show that the integral 4H resonance is due to a dihydrogen ligand (T_1 = 14 ms) while the higher field, integral 2H resonances, is assigned to a hydride (T_1 = 250 ms). The dihydrogen ligands in **5** are likely to be rotating around the M–H_2 axis at low temperature as only one η^2-H_2 environment is observed; this being in accord with findings for other dihydrogen complexes in which the barrier to rotation is very small.[4,50,51] The ^{31}P{^{1}H} NMR spectrum at this temperature is essentially unchanged from that at 298 K. All these findings are consistent with those reported for analogous bisdihydrogen/dihydride complexes, in particular [Rh(PCy$_3$)$_2$(H)$_2$(η^2-H$_2$)$_2$][BAr$^F_4$].[46]

Addition of the hydrogen acceptor tbe to **5** reforms the mixture **2a**/**2b** after 3 h. This is a stepwise process, with the second dehydrogenation much slower than the first, as observed previously for both the synthesis of **2a**/**2b** and the dehydrogenation of PCyp$_3$ in [Ru(PCyp$_3$)$_2$(H$_2$)(η^2-H$_2$)$_2$].[30] The product of the first dehydrogenation can be trapped by addition of acetonitrile immediately after tbe addition, which results in the isolation of **6**, as crystalline material in moderate (53%) yield (Scheme 5); although the reaction is quantitative by NMR spectroscopy. No further dehydrogenation in **6** occurs as the coordinated acetonitrile prevents further dehydrogenation of the other cyclopentyl ring by blocking the vacant site required for C–H activation.

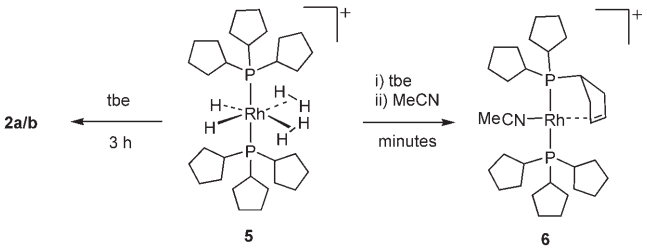

Scheme 5.

The solid-state structure of **6** is shown in Figure 4, and this demonstrates that the molecule adopts an approximate square planar geometry, with *trans* orientated phosphines [P1-Rh-P2 178.02(3)°] and an acetonitrile ligand sitting opposite the alkene double bond on the dehydrogenated PCyp$_3$ ligand [N-Rh-C2/C3$_{midpoint}$ 173.57(8)°]. The molecule thus does not show the distortion observed in **2b**, as expected in the absence of competing *trans* π acceptors (see later). Other bond lengths and angles are as expected. In solution, two ^{31}P environments are observed in the ^{31}P{^{1}H} NMR spectrum of **6**, that also show distinctive *trans* P–P coupling, namely δ 74.6 [dd, J(P,P) = 302, J(Rh,P) = 123 Hz] and 25.7 ppm [dd, J(P,P) = 302, J(Rh,P) = 117 Hz]. The ^{1}H and ^{31}C{^{1}H} NMR spectra show signals due to coordinated MeCN and the alkene. In particular one alkene environment is observed, consistent with the square-planar geometry.

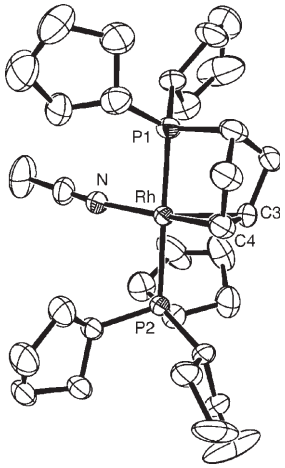

Figure 4. Solid-state structure of **6**. Hydrogen atoms and the [BAr$^F_4$]$^-$ anion are not shown. Thermal ellipsoids are presented at the 50% probability level. Selected bond lengths [Å] and angles [°]: Rh–P1 2.281(1), Rh–P2 2.358(1), Rh–N 2.060(3), Rh–C3 2.136(3), Rh–C4 2.145(3), C3–C4 1.378(5), P1-Rh-P2 178.02(3), P1-Rh-Ct3/4, Ct3/4-Rh-N 173.57(8), P1-Rh-Ct3/4 83.34(2), P1-Rh-N 91.04(8), P2-Rh-Ct3/4 95.14(2), P2-Rh-N 90.55(8).

Computational Studies on 2a and 2b: We have performed DFT calculations on **2a** and **2b** as well as a number of related smaller model systems. Geometry optimisations on the full complexes provided good agreement with experimental data with, in particular, the bent structure of **2b** being well reproduced (the alkene midpoint-Rh-alkene midpoint angle, that we shall call θ being 146° compared with 144° from experiment, see Supporting Information for details). In addition, **2b** was computed to be 7.5 kJ mol^{-1} more stable than **2a**, consistent with the small preference determined from experimental equilibrium concentrations. With smaller models of the type [Rh{PR$_2$(η^2-C$_5$H$_7$)}$_2$]$^+$ (R = H, Me) the

cis form becomes the more stable, by 2.0 kJ mol^{-1} (R = H) and by 0.8 kJ mol^{-1} (R = Me). The different isomeric preferences computed with these various models suggest that the greater stability of the *trans* species in the full system is primarily driven by steric effects.

The main focus of our study at this point, however, was to account for the bent structure of **2b** and to this end we have employed the simplified model system *trans*-[Rh(PH$_3$)$_2$(C$_2$H$_4$)$_2$]$^+$, **2b′**. This species optimises to a bent geometry with $\theta = 146°$ and this was found to be 13.3 kJ mol^{-1} more stable than an alternative square-planar geometry obtained with θ fixed at 180°. The occupied metal-based d orbitals of these two structures are shown schematically in Figure 5.

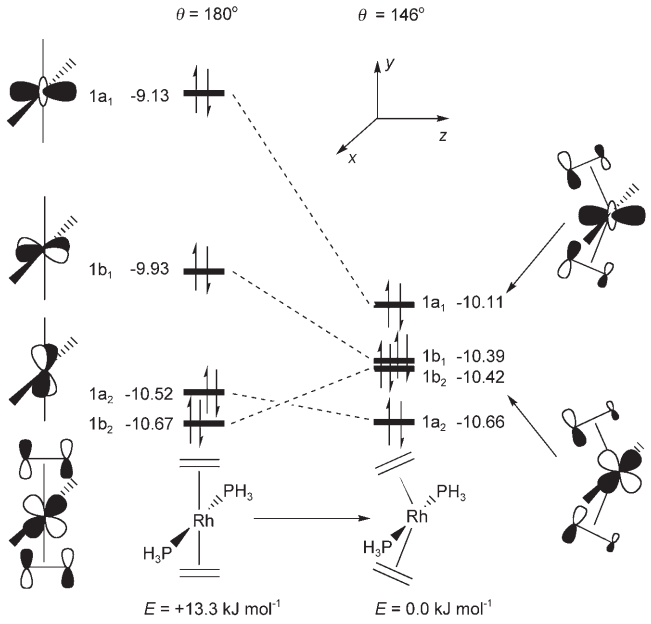

Figure 5. Energy level diagram [eV] for the occupied metal-based d orbitals of **2b′**.

For $\theta = 180°$ the HOMO is dominated by Rh d_{z^2} and s character (>93%). To lower energy the $1b_1$ and $1a_2$ orbitals are again mainly metal-based (ca. 85%), but are now stabilised by mixing with the PH_3 σ* orbitals (contributions omitted from Figure 5). Most stable is the $1b_2$ orbital for which π-back donation to the alkenes is apparent. Reducing θ to 146° results in a strong stabilisation of the $1a_1$ orbital by around 1 eV due to enhanced π-back donation from the Rh d_{z^2} orbital to the alkene π* orbitals. The only destabilisation that occurs upon bending is in the $1b_2$ orbital (0.25 eV) and this arises from both a loss of π-back donation as the Rh-(d_{yz})/alkene(π*) overlap diminishes and the introduction of some σ-antibonding character. Overall, π stabilisation of the $1a_1$ orbital is the dominant effect and this drives the distortion towards a bent structure.

As mentioned previously, the structure of **2b** is reminiscent of that reported for [Ru(CO)$_2$(P*t*Bu$_2$Me)$_2$].[43] In that case a rationalisation in terms of Ru→CO π-back donation was proposed, this being enhanced in the bent form due to the extremely e$^-$ rich Ru^0 centre. Indeed, calculations on isoelectronic (but less e$^-$ rich) [Rh(CO)$_2$(PH$_3$)$_2$]$^+$ favoured a square-planar structure. The structure of **2b**, however, indicates that deformation away from a square-planar geometry in these 16e species can arise not only from the nature of the metal centre but also from the type of the π-acceptor ligand involved. To test this idea we used the ADF program to analyse the M–L interaction in *trans*-[Rh(PH$_3$)$_2$(L)$_2$]$^+$ species (L = C$_2$H$_4$ or CO), where geometries with $\theta = 180$ or 146° were employed. In each case the molecule was split into {Rh(PH$_3$)$_2$L}$^+$ and {L} fragments, with the major point of interest being the extent of π-back donation from the Rh d_{z^2} orbital (the HOMO of the {Rh(PH$_3$)$_2$L}$^+$ fragment) into the π* acceptor orbital on L. From the above discussion this interaction is the one that should control whether a deformation is seen.

The data in Table 1 indicate that for both systems reducing θ leads to increased Rh d_{z^2} L π* overlap, although this effect is notably larger for L = C$_2$H$_4$. We also monitored the change in orbital occupation when the two fragments interact to form the full *trans*-[Rh(PH$_3$)$_2$(L)$_2$]$^+$ species. For $\theta = 180°$ the Rh d_{z^2} (doubly occupied in {Rh(PH$_3$)$_2$L}$^+$) is unaffected, as there is no low-lying orbital of correct symmetry on L with which to interact. When $\theta = 146°$ Rh d_{z^2} → L π-back donation occurs and the greater depopulation of the Rh d_{z^2} in *trans*-[Rh(PH$_3$)$_2$(C$_2$H$_4$)$_2$]$^+$ indicates the improved efficiency of this process with L = C$_2$H$_4$, a direct result of greater Rh d_{z^2}/C$_2$H$_4$ π* overlap. The significant populations of the π* orbitals of both CO and C$_2$H$_4$ when $\theta = 180°$ arise from there being several {Rh(PH$_3$)$_2$L}$^+$ orbitals capable of π-back donation at that geometry. The fact that the population increases further upon bending *trans*-[Rh(PH$_3$)$_2$-(C$_2$H$_4$)$_2$]$^+$ but is unaffected in *trans*-[Rh(PH$_3$)$_2$(CO)$_2$]$^+$ is further evidence of improved π-back donation with the alkene in this system.

Table 1. Computed data from *trans*-[Rh(PH$_3$)$_2$L$_2$]$^+$ fragment calculations.

L/θ [°]	Orbital overlap ⟨Rh d_{z^2}|L π*⟩	Orbital populations	
		Rh d_{z^2}	L π*
C$_2$H$_4$/180	0.001	1.99	0.22
C$_2$H$_4$/146	0.161	1.69	0.32
CO/180	0.001	1.99	0.17
CO/146	0.071	1.95	0.18

Our calculations confirm that enhanced M→L π-back donation promotes the bent geometries seen in some ML$_2$-(PR$_3$)$_2$ species. This effect may arise from either a particularly e$^-$ rich metal centre (as in [Ru(CO)$_2$(P*t*Bu$_2$Me)$_2$]) or the presence of a π-acceptor ligand capable of efficient interaction with the metal d_{z^2} orbital. The alkene ligands in **2b′** (and by extension **2b**) achieve this through improved overlap and this seems simply to be a result of the spatial extent of the π* orbital, which has a well-matched "bite angle" for the metal d_{z^2}. Although CO is normally considered a better π acceptor than an alkene ligand, in this specific case the

shape of the CO π* orbitals do not facilitate a strong enough interaction with the metal d_{z^2} for bending to occur in *trans*-$[Rh(PH_3)_2(CO)_2]^+$. A further requirement for deformation appears to be a *trans* arrangement of two π-acceptor ligands. Thus near-planar structures are observed for *cis* structures such as **2a** and $[Ru(CO)_2(tBu_2PCH_2CH_2PtBu_2)]$.[52] Presumably π-competition effects are more pronounced with a trans arrangement and adds a further driving force to maximise π-back donation by deforming away from a planar structure.

Mono-PCyp$_3$ complexes: The intramolecular dehydrogenation of cyclopentyl groups is also observed in mono-phosphine rhodium complexes. Related complexes based on the tropp^{Ph} ligand set have been previously reported by Grützmacher, although in these cases a preformed phosphine alkene ligand is used.[17,40,41] The synthesis of a suitable precursor material $[RhCl(nbd)(PCyp_3)]$ comes from treatment of $[Rh(nbd)Cl]_2$ with $PCyp_3$. When treated with $Na[BAr^F{}_4]$ in fluorobenzene alkyl dehydrogenation results in formation of the fluorobenzene complex $[Rh(\eta^6\text{-}C_6H_5F)\{PCyp_2(\eta^2\text{-}C_5H_7)\}][BAr^F{}_4]$ **7** (Scheme 6). Use of benzene as co-solvent gives the analogous benzene complex **8**. In the formation of **7** and **8**, the coordinated norbornadiene acts as a hydrogen acceptor, and norbornene is observed in the reaction mixture (by GC and ^{1}H NMR spectroscopy). The ^{1}H and $^{13}C\{^1H\}$ NMR spectra of **7** show signals arising from the coordinated arene, together with a signal characteristic of a coordinated alkene [^{1}H: δ 3.89, ^{13}C: δ 65.04 d, J(Rh,C) = 16 Hz, HC=CH]. Similar signals are observed in the spectra of **8**. Complexes **7** and **8** have similar $^{31}P\{^1H\}$ NMR spectra, with **7** showing additional coupling due to the fluorine on the arene ring [J(F,P) = 3.8 Hz]. The solid-state structures (Figure 6) show that the bond lengths and angles are effectively the same in both complexes, and confirm the presence of a coordinated C=C double bond by short C–C distances [**7** C13–C14 1.401(4); **8** C13–C14 1.389(4) Å], together with M–C distances typical for M–alkene coordination, which are similar to those observed for **2b** and **6**.

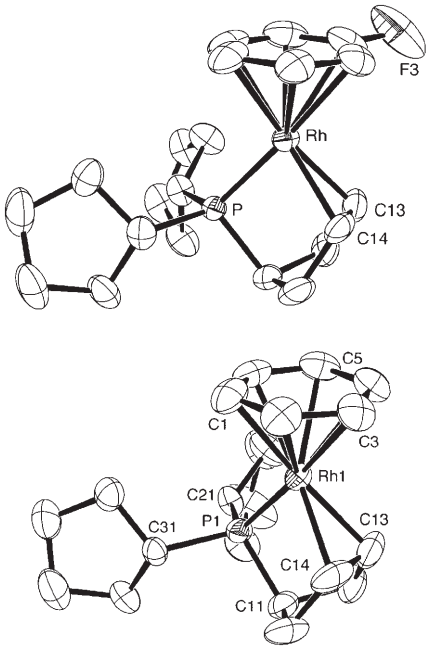

Figure 6. Solid-state structure of **7** (top) and **8** (bottom). Hydrogen atoms and the $[BAr^F{}_4]^-$ anion are not shown. Thermal ellipsoids are presented at the 50% probability level. Selected bond lengths [Å] and angles [°] for **7**: Rh–P 2.2412(6), Rh–C13 2.125(2), Rh–C14 2.128(2), Rh–C1–6 2.244(2)–2.337(3), C13–C14 1.401(4), P-Rh-Ct13/14 82.56(2); for **8**: Rh–P 2.219(3), Rh–C13 2.133(6), Rh–C14 2.114(4), Rh–C1–6 2.250(2)–2.336(2), C13–C14 1.414(5), P-Rh-Ct13/14 82.93(8).

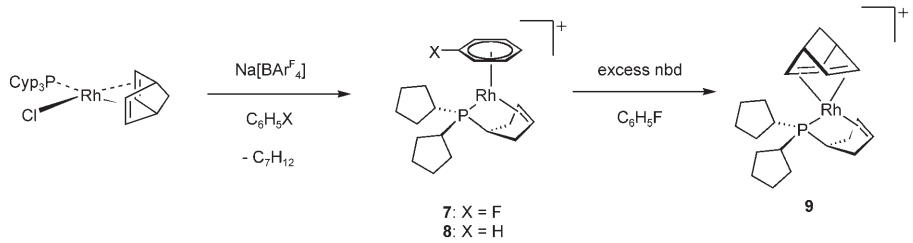

Scheme 6.

Adding an excess of nbd to **7** affords the nbd adduct $[Rh(nbd)\{PCyp_2(\eta^2\text{-}C_5H_7)\}][BAr^F{}_4]$ (**9**) in which the diene has replaced the fluorobenzene. The NMR data for **9** show the presence of three-coordinated alkene groups and, aided by coupling patterns and ^{1}H,^{13}C correlation experiments, these have been assigned to specific alkene groups (see Experimental Section). The $^{31}P\{^1H\}$ NMR spectrum shows the distinctive downfield shift of the coordinated phosphine ligand to δ 73.1 ppm [$\Delta\delta$ +60 compared with **1**]. The solid-state structure of **9** is shown in Figure 7 and confirms the coordinated nbd ligand. Bond lengths and angles of the dehydrogenated phosphine ligand are similar to the other complexes reported here. The complex is distorted away from square-planar, as observed for **2b**, so that the mid-points of two of the alkene ligands [C1/C2 and C13/C14] do not lie rigorously *trans* to one another but instead describe an angle of 153.16(1)° around Rh. The angle P-Rh-C4/C5 is close to linear [175.25(2) deg]. As for **2b** this distortion is a consequence of two *trans* π-accepting ligands.

For the complexes **7** and **8** the mechanism of dehydrogenation most likely follows, in part, that outlined in Scheme 3. Halide abstraction from $[RhCl(nbd)(PCyp_3)]$ would afford intermediate **A**. The pathway diverts after intermediate **C**, as the absence of a second phosphine ligand results in a highly unsaturated molecule that coordinates with the arene solvent to form the obtained products.

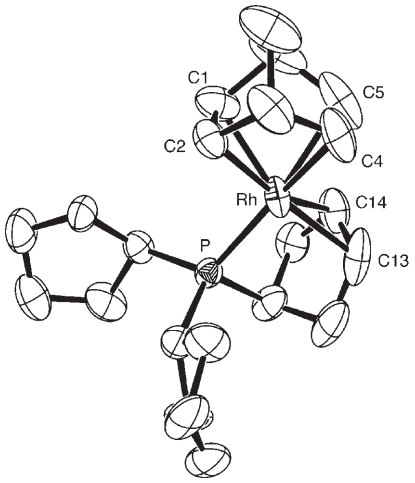

Figure 7. Solid-state structure of **9**. Hydrogen atoms and the $[BAr^F_4]^-$ anion are not shown. Thermal ellipsoids are presented at the 50% probability level. Selected bond lengths [Å] and angles [°]: Rh–P 2.2694(7), Rh–C1 2.158(4), Rh–C2 2.158(3), Rh–C4 2.262(3), Rh–C5 2.253(4), Rh–C13 2.224(4), Rh–C14 2.247(3), C1–C2 1.365(5), C4–C5 1.357(6), C13–C14 1.369(5); P-Rh-Ct4/5 175.25(2), P-Rh-Ct1/2 106.01(2), P-Rh-Ct13/14 82.86(2), Ct1/2-Rh-Ct4/5 69.50(1), Ct1/2-Rh-Ct13/14 153.16(1), Ct4/5-Rh-Ct13/14 101.86(1).

Acceptorless dehydrogenation: Up to this point all the dehydrogenations reported have been facilitated by a hydrogen acceptor, either norbornene or *tert*-butylethene. The systems under discussion here also can undergo acceptorless alkyl dehydrogenation, by changing the supporting ligand set from nbd to dppe. Acceptorless dehydrogenation is potentially more interesting as it is more atom efficient, and systems that perform this process catalytically on alkanes have been reported.[7,53,54]

Addition of $Na[BAr^F_4]$ to $[RhCl(dppe)(PCyp_3)]$ results in the quantitative formation (by NMR spectroscopy) of $[Rh(dppe)\{PCyp_2(\eta^2\text{-}C_5H_7)\}][BAr^F_4]$ (**10**) (Scheme 7). Complex

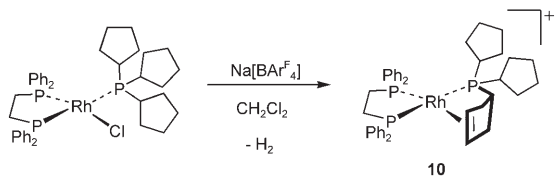

Scheme 7.

10 is isolated as an analytically pure solid in 61% yield. This reaction occurs in 5 minutes in CD_2Cl_2 solution. The ^1H NMR spectrum of **10** shows a signal attributable to a coordinated alkene at δ 4.89, which shows one-bond correlation to a signal at δ 96.2 in the $^{13}C\{^1H\}$ NMR spectrum, fully consistent with a coordinated alkene. The hydride region of the ^1H NMR spectrum is featureless—indicating the absence of Rh–H species. The $^{31}P\{^1H\}$ NMR spectrum shows three signals, all doublet of doublet of doublets, two with characteristically large *trans* P–P coupling [J(P,P) = 283 Hz]. They appear as a tightly coupled ABMX multiplet, with the outer lines of the multiplets significantly reduced in intensity (see Supporting Information). ^1H,^{31}P correlation spectroscopy allows the identification of the ^{31}P resonances and shows that one of the dppe phosphines and the cyclopentylphosphine are *trans*-orientated, as expected from simple geometric considerations. In the solid-state (Figure 8) the presence

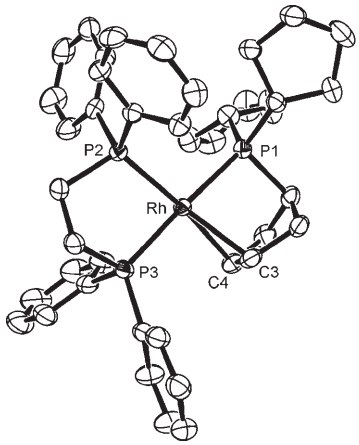

Figure 8. Solid-state structure of **10**. Hydrogen atoms and the $[BAr^F_4]^-$ anion are not shown. Thermal ellipsoids are presented at the 50% probability level. Selected bond lengths [Å] and angles [°]: Rh1–P1 2.3284(5), Rh1–P2 2.2818(5), Rh1–P3 2.2709(5), Rh1–C3 2.242(2), Rh1–C4 2.241(2), C3–C4 1.372(3), P1-Rh1-P2 100.07(2), P1-Rh1-P3 174.42(2), P2-Rh1-P3 83.82(2), P1-Rh1-Ct3/4 83.62(2), P2-Rh1-Ct3/4 172.16(2), P3-Rh1-Ct3/4 93.01(2).

of a coordinated C=C double bond was confirmed by a short C–C distance [C3–C4 1.372(3) Å] together with M–C distances typical for M–alkene coordination [namely 2.241(2), 2.242(2) Å]. Additionally (given the usual caveats regarding the location of hydrogens by X-ray diffraction), only one hydrogen for C3 and C4, respectively, was located in the final difference map. The complex approaches square planar (sum of angles around the Rh = 360.5°, P2-Rh-C3/$C4_{centroid}$ 172.16(2), P1-Rh-P3 174.42(2)].

Addition of H_2 (4 atm 15 minutes or 1 atm 45 minutes) to **10** in CD_2Cl_2 solution results in an uptake of H_2 and the formation of the dihydrogen/dihydride complex $[Rh(dppe)(PCyp_3)(H)_2(\eta^2\text{-}H_2)][BAr^F_4]$ (**11**; see Scheme 8) as the only observable product by NMR spectroscopy. We have not been able to grow suitable crystals of **11** for a solid-state analysis, but the NMR data are unequivocal in its characterization. At room temperature a broad ^{31}P signal is observed,

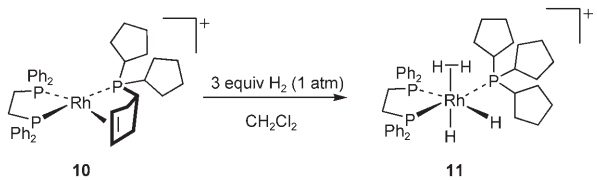

Scheme 8. 3 equiv H_2 (1 atm).

and a very broad signal at $\delta = -4.5$ ppm ($\approx$2.5 H, fwhm 1800 Hz) is observed in the ^{1}H NMR spectrum. Cooling to 220 K reveals a tightly coupled ABMX system in the $^{31}P\{^1H\}$ NMR spectrum (see Supporting Information) that clearly shows *trans* $^{31}P,^{31}P$ coupling [$J(P,P_{trans}) = 285$ Hz] between one of the dppe phosphines and $PCyp_3$. The ^{1}H NMR spectrum at this temperature displays three signals in the hydride region at $\delta = -3.1$ (2 H), -8.5 (1 H) and -13.0 ppm (1 H). T_1 relaxation times determined for these signals (at 180 K and 400 MHz) identify the integral 2 H signal as being due to a dihydrogen ligand ($T_1 = 19$ ms) while the two integral one signals are clearly due to hydrides ($T_1 = 215$ and 250 ms). The former hydride signal shows a large coupling to ^{31}P [J(P,H) = 149 Hz], placing it *trans* to one of the phosphorus atoms. The signal due to the alkene that is observed in **10** has disappeared in both the ^{1}H and $^{13}C\{^1H\}$ NMR spectra of **11**. These data allow the structure of **11** to be determined as one in which the alkene has been hydrogenated, the phosphorus ligands lie meridional, and the dihydrogen ligand sits *trans* to the high *trans* influence hydride ligand.[46–48] Addition of D_2 to **10** resulted in the incorporation of D_2 in the cyclic alkane (^{2}H NMR, 298 K, $\delta = 1.57$); while addition of D_2 (1 atm) to **11** resulted in rapid H/D exchange, evidenced by a diminution in the intensity of the hydride signals, and the observation of dissolved HD [1:1:1 triplet at δ 4.30, J(D,H) = 43 Hz]. Compound **11** (and **5**) add to the relatively small number of dihydrogen complexes of rhodium known $[Rh(PR_3)_2(H)_2(\eta^2\text{-}H_2)_2][BAr^F{}_4]$ (R = *i*Pr, Cy),[46] $[RhCp^*(H)(\eta^2\text{-}H_2)(PMe_3)]^+$,[55] $[RhTp(H)(\eta^2\text{-}H_2)(PPh_3)]^+$,[56] $RhTp(H)_2(\eta^2\text{-}H_2)$,[57] $Rh(\eta^2\text{-}H_2)(PCP)$,[54] $[Rh(H)_2(\eta^2\text{-}H_2)(PPP)]^+$[58] and $[RhCp^*(\eta^2\text{-}H_2)(dmpm)]^{2+}$[59] [Cp* = η^5-C_5Me_5, Tp = $HB(pz)_3$ or derivative thereof, PCP = η^3-C_6H_3-1,3-$(PtBu_2)_2$, PPP=$MeC(CH_2PPh_2)_3$]. It is also closely related to the isoelectronic neutral complexes $Ru(PPh_3)_3(H)_2(\eta^2\text{-}H_2)$,[60] $Ru(dtbpmb)(H)_2(\eta^2\text{-}H_2)$[61] [dtbpmb = 1,3-bis((di-*tert*-butylphosphino)methyl)benzyl)] that have been identified as a containing a dihydrogen ligand.

Although complex **11** is stable under 1 atm of H_2 for 24 h in CH_2Cl_2 solution, removal of H_2 under vacuum by freeze/pump/thaw of the solution results in the regeneration of **10**, by sequential H_2 loss from the metal and dehydrogenation of one of the $PCyp_3$ rings. This process is relatively rapid (60 minutes, 298 K) and occurs *without* the addition of an H_2 acceptor. It is not quantitative, with about 70% of **10** (by NMR spectroscopy) being recovered, with the remainder being unidentified decomposition products. The hydrogen loss under a vacuum means that we have not been able to quantify the H_2 loss experimentally or observe free H_2 in solution.

We have, however, been able to observe intermediates in this dehydrogenation process by placing **11** briefly (seconds) under a vacuum at 77 K and then warming, which removes only the bound H_2 ligand. The $^{31}P\{^1H\}$ NMR spectrum at 298 K shows a broad signal, while the high field region of the ^{1}H NMR spectrum displays a very broad signal at δ -4.5. Cooling to 180 K results in a $^{31}P\{^1H\}$ NMR spectrum that shows an ABMX pattern with *trans* phosphines (as for **11**). Two broad hydride signals are observed in the ^{1}H NMR spectrum at δ -8.4 and -20.5 ppm at this temperature, that coalesce at 250 K indicating a fluxional process that exchanges the hydrogen ligands (see Supporting Information). These data are consistent with the structure presented for **12** (Scheme 9) that suggests an agostic interaction from the cyclopentyl ligand. The highest field hydride chemical shift is assigned to the hydride *trans* to the lightly stabilized site, as it is well established that the chemical shift of hydride is sensitive to the *trans* ligand.[62] No evidence for an agostic C–H interaction was seen, and although such interactions are often highly fluxional, we cannot discount the possibility that **12** is a solvent (i.e., CD_2Cl_2) or adventitious water complex. When **12** is placed under extended vacuum it changes to **10**, indicating that it is a possible intermediate on the dehydrogenation cycle. Addition of MeCN to **12** gives $[Rh(dppe)(PCyp_3)(H)_2(MeCN)][BAr^F{}_4]$ (**13**) (Scheme 10) which is spectroscopically characterized as a complex in which the acetonitrile has replaced the putative agostic interaction in **12**. Key spectroscopic markers for **13** are two hydride resonances at δ -8.94 and -17.99 ppm, one of which shows coupling to a *trans* phosphine [δ -8.94,

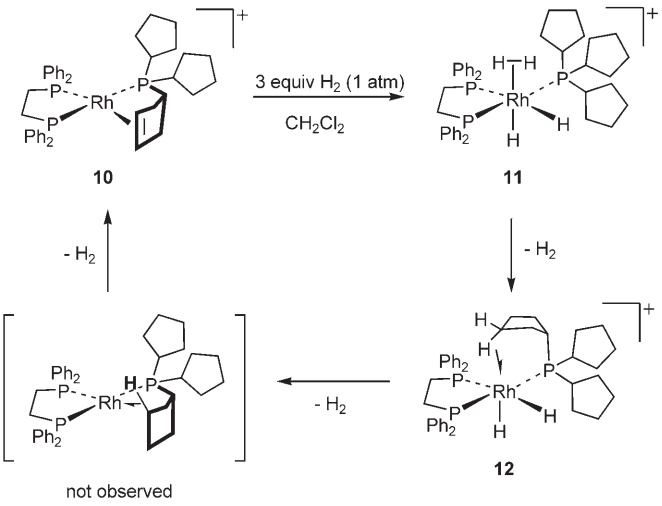

Scheme 9. 3 equiv H_2 (1 atm).

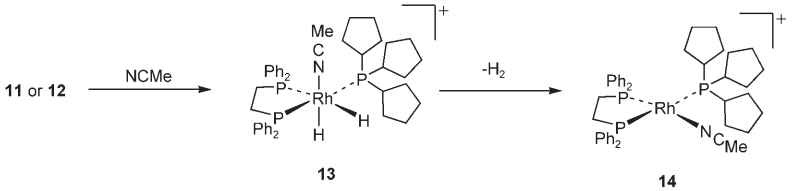

Scheme 10.

ddd, J(P,H) = 160, J(Rh,H) = 14, J(H,H) = 14 Hz], and an ABMX pattern in the $^{31}P\{^1H\}$ NMR spectrum that shows *trans* PP coupling [J(P,P) = 319 Hz]. Under an Ar atmosphere, complex **13** loses H_2 in solution over 24 h to afford the rhodium(I) complex [Rh(dppe)($PCyp_3$)(MeCN)][BAr^F_4] (**14**). Complex **14** has been fully characterised, including by single crystal X-ray crystallography (see Supporting Information). The bound MeCN in **14** blocks alkyl phosphine dehydrogenation and it remains unchanged at room temperature for days, similar to **6**. Complex **14** can also be accessed by direct addition of MeCN to **11**.

Comparison between cyclopentylphosphine and cyclohexylphosphine: Given the ease of dehydrogenation of $PCyp_3$ the question arises as to whether tris(cyclopentylphosphine) is a particularly privileged motif for this transformation, and we have studied this experimentally and computationally by comparison with tris(cyclohexylphosphine) analogues. Cyclohexylphosphines are established to undergo dehydrogenation in the presence of a hydrogen acceptor,[13,14] and thus the comparison is a useful one. The experimental evidence is presented first, and two sets of experiments demonstrate clearly that the cyclopentyl motif undergoes alkyl dehydrogenation significantly faster than cyclohexyl.

Treatment of [RhCl(dppe)(PCy_3)] with Na[BAr^F_4] in CD_2Cl_2 does not result in dehydrogenation, in contrast to the $PCyp_3$ analogue. Instead a highly fluxional molecule, **15**, is formed, as tentatively characterised in solution, which adds MeCN to form the stable adduct [Rh(dppe)(PCy)(MeCN)][BAr^F_4] **16**, which has been characterised unambiguously by NMR spectroscopy (Scheme 11). Despite repeated attempts we have not been able to grow suitable crystals of the fluxional intermediate complex **15**, and characterisation rests on spectroscopic data alone. Room temperature NMR data show broad peaks, that on cooling (180 K) sharpen but afford a complex mixture of products. Adding MeCN to this solution at room temperature produces a single, non-fluxional, complex in quantitative yield by NMR spectroscopy, identified by NMR spectroscopy and ESI-MS as the adduct **16**. We suggest the most plausible explanation for these data, and the observed reactivity with MeCN, is a structure for **15** that either invokes an agostic C–H interaction between the cyclohexyl group and the metal, or one in which solvent (CD_2Cl_2) or trace, adventitious, water coordinate to the fourth site of the square-planar rhodium(I). The data cannot discriminate between these possibilities and it is likely that a mixture of these complexes exists in solution. Whatever the precise structure, important for the comparison with the $PCyp_3$ complex is that no dehydrogenation has occurred and the interaction in the fourth coordination site is sufficiently weak as to be readily displaced by MeCN. Addition of tbe to **15** does not induce C–H activation and only gradual decomposition to unidentified products occurs over 24 h.

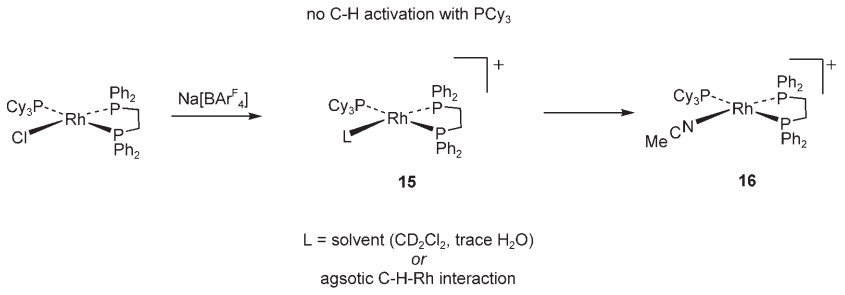

Scheme 11.

The relative ease of acceptorless dehydrogenation of $PCyp_3$ compared with PCy_3 is demonstrated even more clearly in a competition experiment using the mixed alkyl phosphine PCy_2Cyp; the synthesis from PCy_2Cl and BrMgCy being described in the Experimental Section. This phosphine provides the metal a choice of cyclopentyl or cyclohexyl groups, assuming that rotation around the Rh–P bond is a relatively low-energy process. A suitable precursor complex [RhCl(nbd){PCy_2Cyp}] is readily synthesised, and treatment with Na[BAr^F_4] in C_6H_5F results in dehydrogenation and the formation of only *one* complex in quantitative yield (by NMR spectroscopy), identified spectroscopically as [Rh(η^6-C_6H_5F){$PCy_2(\eta^2$-$C_5H_7)$}][BAr^F_4] (**17**) in which the cyclopentyl ligand has exclusively (by the detection limits of NMR spectroscopy) undergone alkane dehydrogention, leaving the cyclohexyl groups intact (Scheme 12). In our hands, it was not possible to obtain analytically pure material of **17** due to decomposition in solution. Adding toluene to the reaction mixture resulted in the formation of [Rh(η^6-C_6H_5Me){$PCy_2(\eta^2$-$C_5H_7)$}][BAr^F_4] (**18**) that is more stable and could be isolated as crystalline material in 61% yield. ^1H, $^{31}P\{^1H\}$ NMR spectroscopy and X-ray crystallography (the last for **18** only) have been used to characterise these complexes. In particular the $^{31}P\{^1H\}$ NMR spectra of the crude reaction mixture shows only one complex (see Supporting Information), demonstrating that the dehydrogenation is selective. The NMR data for **17** and **18** are very similar to **7** and **8** and

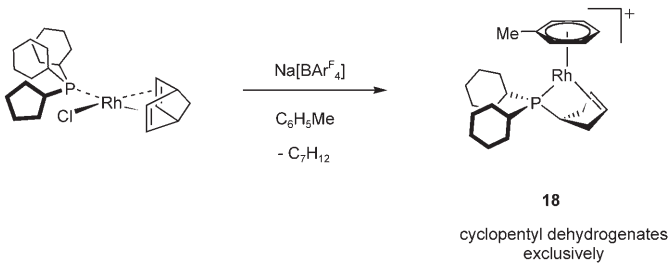

Scheme 12.

indicate a molecule with C_s symmetry (i.e., one alkene environment and three arene environments in the ratio 1:2:2). As dehydrogenation of one of the cyclohexyl groups would break the symmetry to C_1[13] this is strongly suggestive of selective dehydrogenation of the cyclopentyl ring. The solid-state structure of **18** is shown in Figure 9 and confirms this. Bond lengths and angles are unremarkable and close to those in **7**, **8** and **9**.

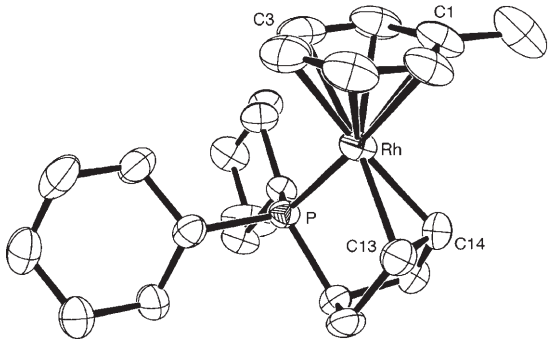

Figure 9. Solid-state structure of **18**. Only the major disorder component is shown. Hydrogen atoms and the $[BAr^F_4]^-$ anion are not shown. Thermal ellipsoids are presented at the 50% probability level. Selected bond lengths [Å] and angles [°]: Rh–P 2.2348(11), Rh–C13 2.138(3), Rh–C14 2.123(5), Rh–C1–6 2.243(4)–2.338(4), P-Rh-Ct13/14 81.86(3).

Computed energy profiles for the dehydrogenation of 13 and 16: We have used DFT calculations to model the mechanism of dehydrogenation of a cyclopentyl group in the putative intermediate complexes $[Rh(dppe)(PCyp_3)]^+$ (**19**) and a cyclohexyl group in $[Rh(dppe)(PCy_3)]^+$ (**20**), the species formed upon halide removal from $[Rh(dppe)Cl(PR_3)]$. In the following we discuss the results obtained with small model systems of the type $[Rh(H_2PCH_2CH_2PH_2)(PH_2R)]^+$ (R = Cyp, **19′**, or Cy, **20′**, Scheme 13). We have also recom-

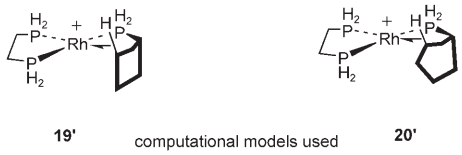

Scheme 13.

puted several of the key stationary points using the full experimental systems, however, these test calculations showed the introduction of the full phosphine substituents to have a minimal impact on the computed energetics of reaction (see Supporting Information for full details).

Details of the initial C–H activation processes computed for **19′** and **20′** are shown in Figure 10. The computed structure of **19′** shows an agostic interaction between the Rh centre and the C3–H bond of the cyclopentyl substituent. Attempts to locate alternative non-agostic species were unsuccessful, with all optimisations reverting to the structure shown in Figure 10. From **19′** C–H activation proceeds with an activation barrier of only 9.9 kcal mol^{-1} and leads directly to a rhodium(III)–alkyl hydride intermediate, **I2′** (E = −0.5 kcal mol^{-1}). Complex **I2′** also features an agostic interaction with the cyclopentyl C4–H bond. For **20′** C–H activation entails a slightly higher computed barrier of 13.6 kcal mol^{-1} and, unlike the equivalent process from **19′**, the initial intermediate formed (**I1′**, E = +7.1 kcal mol^{-1}) does not feature an agostic interaction. A similar distinction can also be seen in the C–H activation transition states, where for **TS(19′-I2′)** an incipient agostic interaction with the C4–H bond is already apparent (Rh···H 2.47 Å; C4–H 1.11 Å), while in **TS(20′-I1′)** the equivalent RhLH distance is over 3.0 Å. The presence of this stabilizing secondary agostic interaction in **TS(19′-I2′)** may lie behind the slightly lower C–H activation barrier from **19′** compared to **20′**. The absence of an equivalent interaction in **TS(20′-I1′)** is due to the chair conformation of the cyclohexyl substituent, which ensures that the C4–H bonds initially must remain remote from the metal centre upon C-H activation. Before β-H transfer can occur in **I1′**, a second process corresponding to a conformational change of the ring from a chair to a twist-boat form is required. This entails a minimal activation barrier of 1.8 kcal mol^{-1} and gives an agostically-stabilised intermediate **I2′**, analogous to that derived from **19′**. Complex **I2′** is 5.3 kcal mol^{-1} less accessible for the Cy system than in the Cyp system and this presumably reflects the enforced twist-boat conformation of the cyclohexyl ring.

From the intermediates **I2′**, formation of the final dehydrogenation products requires sequential β-H transfer and H_2 loss (see Figure 11). Focussing on the Cyp model, β-H transfer in **I2′** proceeds with a barrier of 8.0 kcal mol^{-1} to generate the *trans*-dihydride *trans*-**I3′** (E = +5.1 kcal mol^{-1}). Loss of H_2 necessitates isomerisation to *cis*-**I3′** and the transition state for this process, **TS(*trans–cis*)-I3′** (E = +21.7 kcal mol^{-1}), corresponds to an intramolecular trigonal twist rearrangement. A similar *trans* to *cis* isomerisation has been previously computed.[44] Reductive elimination of H_2 from *cis*-**I3′** is found to be a two-step process, involving the initial formation of a dihydrogen complex before H_2 dissociation to form **10′**. The latter H_2 loss step has the higher-lying transition state (**TS(*cis*-I3′-10′)**, E = +5.2 kcal mol^{-1}) and this is indicated in Figure 11. Details of the other stationary points involved are provided in the Supporting Information. The computed structure of **10′** is in reasonable agreement with that determined experimentally for **10**, although the calculations tend to overestimate the Rh-P distances.[63] Overall, dehydrogenation of **19′** to form **10′** is computed to be endothermic by 3.9 kcal mol^{-1}, although the inclusion of entropic effects associated with H_2 loss make the free energy change favourable by 2.3 kcal mol^{-1}. Taking the data presented in Figures 10 and 11 together indicates that the overall rate determining step for dehydrogenation is associated with the *trans–cis* isomerisation and this corresponds to an overall activation energy of 21.7 kcal mol^{-1}. For the cyclohexyl model the computed β-H transfer/H_2 loss reaction profile is very

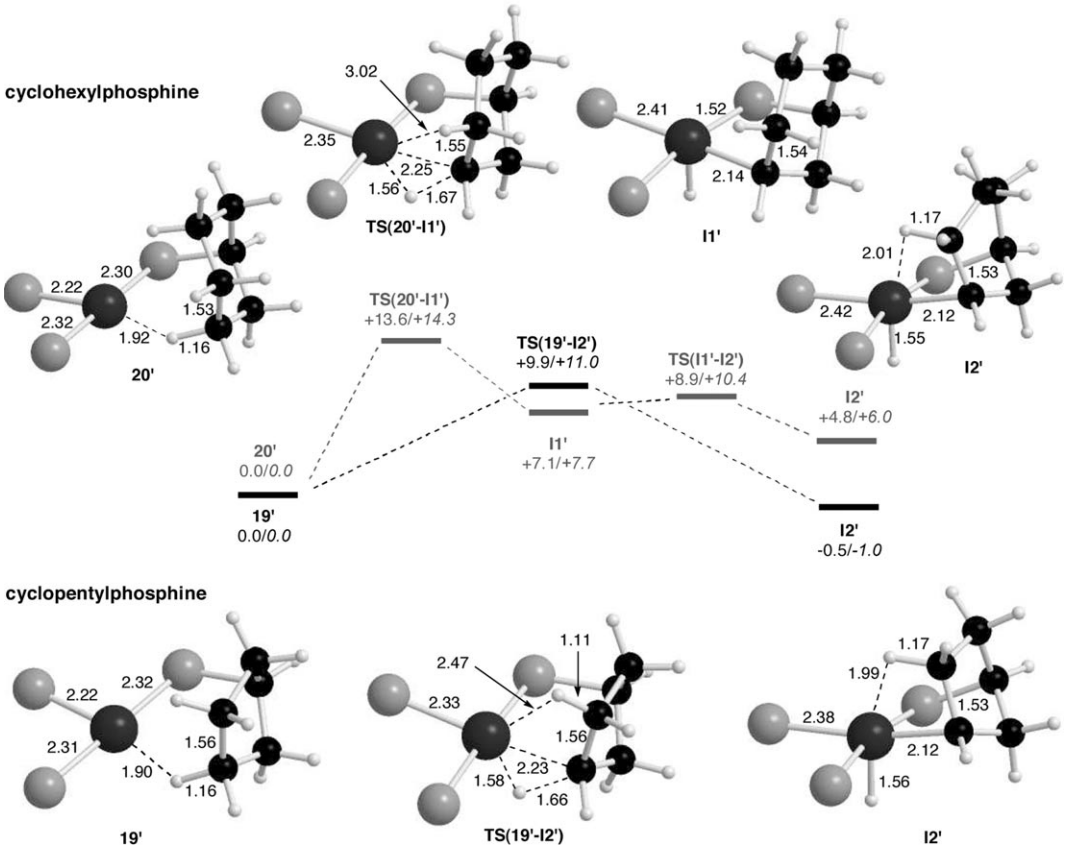

Figure 10. Computed reaction profiles [kcal mol^{-1}] for C-H activation in **19′** (bottom) and **20′** (top, grey). Values include a correction for zero-point energy and free energies are shown in italics. Geometries with key distances [Å] are given for selected stationary points with non-participating phosphine substituents being omitted for clarity. Details of **TS(I1′-I2′)** are supplied in the Supporting Information.

similar to that described above for the cyclopentyl species, with the exception that it is consistently around 5 kcal mol^{-1} higher in energy.[64] Dehydrogenation is therefore less favourable for **20′** than for **19′**, both thermodynamically ($\Delta E = +7.2$ kcal mol^{-1}, $\Delta G = +1.0$ kcal mol^{-1}) and kinetically ($\Delta E^{\ddagger} = +27.5$ kcal mol^{-1}).

The lower computed barrier for dehydrogenation of **19′** compared to **20′** is consistent with the greater propensity of cyclopentylphosphines to undergo dehydrogenation seen experimentally and, in particular, the fact that dehydrogenation occurs upon halide abstraction from [Rh(dppe)(PCyp$_3$)Cl], but not from [Rh(dppe)(PCy$_3$)Cl]. However, the calculations also suggest that the initial C–H activation and β-H transfer steps in the dehydrogenation process should be accessible for both systems, although the barriers for these processes are again lower for a cyclopentyl rather than a cyclohexyl substituent. This may account for the selective dehydrogenation of the C5 ring in [RhCl(nbd){PCy$_2$Cyp}] described above, where the presence of a hydrogen acceptor may negate the need for the high energy *trans–cis* isomerisation step. For **19** the identification of an intramolecular isomerisation (and not C–H bond cleavage) as the rate determining step in the dehydrogenation process should be amenable to testing via measurement of the k_H/k_D kinetic isotope effect on the rate of reaction of **19** and its perdeuterio-analogue [Rh(dppe){P(C$_5$D$_9$)}$_3$]$^+$. Experimental studies are needed to verify this.

In the light of the above results, a number of reasons can be put forward to account for the greater susceptibility of a cyclopentylphosphine ligand towards dehydrogenation compared to a cyclohexylphosphine analogue. Initial C–H activation step is more accessible with a cyclopentyl substituent, as its geometry allows secondary stabilising agostic interactions to develop in the transition state involved. Moreover the β-agostically stabilised intermediate formed is more stable as the C5 ring does not require any conformational change, whereas with a cyclohexyl substituent a twist-boat conformation is required (see **I2′** above). The energetics of the subsequent β-H transfer and H$_2$ loss are very similar for the cyclopentyl and cyclohexyl species and so the higher energies computed for all the phosphine–cyclohexene stationary points must reflect an intrinsic destabilization associated with that ligand. Part of this preference is derived from the cycloalkanes themselves, as at the level of theory used here the energy of dehydrogenation of cyclopentane is slightly lower than that of cyclohexane (+25.0 compared with +26.4 kcal mol^{-1}). In addition the phosphine–cyclohexene ligand generally exhibits slightly longer Rh–C(alkene) bonds than in the phosphine–cyclopentene analogues, suggesting that the C6 ligand does not bind as strongly. This idea was

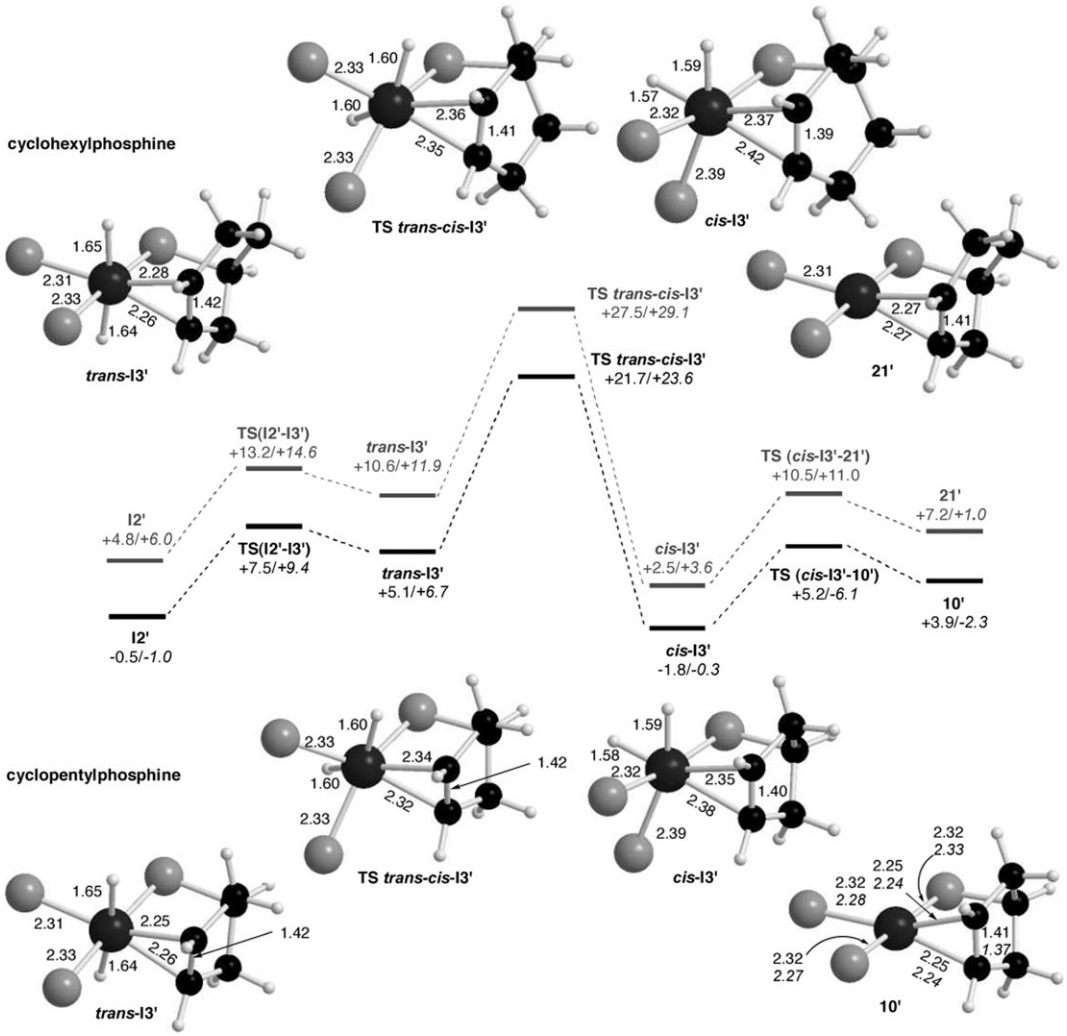

Figure 11. Computed reaction profiles for β-H transfer and H_2 loss from intermediate **I2′** resulting from **19′** (bottom) and **20′** (top, grey). Values include a correction for zero-point energy and free energies are shown in italics. Geometries with key distances [Å] are given for selected stationary points with non-participating phosphine substituents being omitted for clarity. For **10′** selected experimental distances are given for comparison while full details of all other stationary points are supplied in the Supporting Information.

confirmed by computing the energy required to dissociate the alkene arm in the two *cis*-**I3′** intermediates, a process that was 2.1 kcal mol^{-1} easier for the phosphine–cyclohexene species.

Conclusion

We have demonstrated experimentally and computationally that dehydrogenation in cyclopentylphosphine ligands is a process that occurs readily, presenting examples of dehydrogenation in the presence or absence of a hydrogen acceptor. This transformation is promoted by a facile initial C-H activation step in which a supporting, secondary agostic interaction may stabilize the transition state. In addition, acceptorless dehydrogenation is promoted by the greater accessibility of the phosphine–cyclopentene ligand and its greater ability to stabilize Rh^I centres compared to its phosphine–cyclohexene analogues. The ease of this transformation suggests that cyclopentylphosphines are unlikely to be completely innocent ligands in organometallic chemistry. This is not necessarily a detrimental transformation, as the concise generation of mixed phosphine/alkene ligands on a cationic rhodium(I) metal centre may have application in catalysis, and we have reported initial encouraging results that point to this.[28]

Experimental Section

General: All manipulations were carried out using standard Schlenk line and glove-box techniques under an inert atmosphere of argon or nitrogen, except when otherwise stated. Glassware was oven dried at 130 °C overnight and flamed under vacuum prior to use. CH_2Cl_2 and pentane were dried over activated alumina, copper and molecular sieves using an M. Braun solvent purification system. CD_2Cl_2 and fluorobenzene were distilled under vacuum from CaH_2. Hydrogenation procedures were carried out at 4 atm hydrogen, by the following procedure: The entire flask

or NMR tube, both equipped with a J. Youngs tap, was frozen in liquid N_2, the flask was pumped down and backfilled with hydrogen (1 atm) and sealed. The solution was allowed to warm to room temperature, resulting in an internal pressure of ca. 4 atm (298:77 $\approx$4). ^{1}H, ^{31}P{^{1}H}, ^{13}C{^{1}H} and HMQC NMR spectra were recorded on Bruker Avance 300 MHz and Bruker Avance 400 MHz and 500 MHz spectrometers. Residual protio solvent was used as reference for ^{1}H NMR spectra (CD_2Cl_2: δ 5.33). Chemical shift values are quoted in ppm and coupling constants are quoted in Hz. NMR analyses were carried out at 298 K unless otherwise stated. Gas chromatography was performed using a Perkin-Elmer GC, helium carrier gas (12 psi), injection volume 0.2 μL, oven temperature 40 °C and a flame ionisation detector. Data was analysed using the TurboChrom software package. $PCyp_3$,[34] and [Rh(nbd)Cl]$_2$[65] were prepared using literature methods. The preparation of [Rh(nbd)(PCy_3)Cl], [Rh(dppe)($PCyp_3$)Cl], [Rh(dppe)(PCy_3)Cl], [Rh(nbd)Cl{PCy_2Cyp}] and P(Cy)$_2$(Cyp) are reported in Supporting Information.

Computational details: The majority of the calculations reported in this paper were run with Gaussian 03.[66] In all cases full density functional theory (DFT) calculations were employing using the BP86 functional. Rh and P centres were described with the Stuttgart RECPs and associated basis sets[67] with a set of d-orbital polarisation functions on P (ζ = 0.387).[68] 6-31G** basis sets were used for all other atoms.[69,70] All stationary points were fully characterized via analytical frequency calculations as either minima (all positive eigenvalues) or transition states (one imaginary eigenvalue). Energies include a correction for zero-point energies and free energies are quoted at 298.15 K. The calculations performed for the analysis of the structure of **2b** employed the ADF2004.01 program. The BP86 functional was again used along with a triple-ζ basis set for Rh and double-ζ plus polarization basis sets for all other atoms. The frozen core approximation was employed for Rh (3d), P (2p), C and O (1s) and relativistic effects were included through the ZORA approximation.[71,72]

X-ray crystallography: Arbitrary hemispheres of intensity data were collected at 150 K on a Nonius Kappa CCD, using graphite monochromated $Mo_{K\alpha}$ radiation (λ = 0.71073 Å). Data were processed using the supplied Nonius software. Structure solution, followed by full matrix least squares refinement on F^2 (all data) was performed using SHELX97[73] under the WINGX 1.70[74] package, after using SORTAV[75] for absorption correction. In each structure some disorder of the cyclopentyl groups was evident, as was disorder of some of the CF_3 groups in the $[BAr^F_4]^-$ anion. For the majority of structures one of the unfunctionalised cyclopentyl rings was disordered over two sites, but this can be satisfactorily modelled in all cases. Figures show only the major component of the disorder. Table 2 gives details of data collection and refinement for the structurally characterised complexes reported.

CCDC 651267 (**2a**), 651268 (**4**), 651269 (**6**), 610376 (**7**), 610375 (**8**), 651270 (**9**), 610374 (**10**), 638584 (**14**), and 651271 (**18**) contain the supplementary crystallographic data for this paper. These data can be obtained free of charge from The Cambridge Crystallographic Data Centre via www.ccdc.cam.ac.uk/data_request/cif.

[($PCyp_3$)$_2$Rh(nbd)][BAr^F_4] (1): A hexane solution of $PCyp_3$ (0.11 mL, 0.42 M, 0.046 mmol) was added to a solution of [Rh(nbd)Cl]$_2$ (50 mg, 0.0108 mmol) in CH_2Cl_2 (15 mL) and the solution was stirred for 15 min. Na[BAr^F_4] (191 mg, 0.0215 mmol) was added, followed by degassed H_2O (15 mL). The two phase mixture was stirred vigorously for 1 h. The mixture was separated and pentane was added to the red-orange (lower) phase until a precipitate began to appear. The flask was placed in the freezer (−20 °C) overnight, and the resulting precipitate was collected by filtration and was washed with pentane. The solid was dried in vacuo to give **1** as yellow-orange crystals (250 mg, 76 %). ^{1}H NMR (400.1 MHz, CD_2Cl_2): δ = 7.72 (s, 8H, BAr^F_4), 7.55 (s, 4H, BAr^F_4), 4.87 (s, 4H, nbd HC=CH), 3.89 (s, 2H, nbd CH), 1.25–2.25 ppm (m, 56H, nbd CH_2 and $(C_5H_9)_3$); ^{31}P{^{1}H} NMR (161.9 MHz, CD_2Cl_2): δ = 13.35 ppm [d, J(P,P) = 147 Hz]; ^{13}C{^{1}H} NMR (100.6 MHz, CD_2Cl_2, 250 K): δ = 161.9 [q, J(B,C) = 50 Hz, BAr^F_4], 134.5 (s, BAr^F_4), 128.5 [qq, J(F,C) = 31, J(B,C) = 2.9 Hz, BAr^F_4], 125.5 [q, J(F,C) = 272 Hz, BAr^F_4], 117.0 (s, BAr^F_4), 71.9 (m, CH=CH), 67.5 (m, nbd CH_2), 52.5 (m,

Table 2. X-ray crystallographic data collection and refinement details.

	2b	**4**	**6**	**7**	**8**	**9**	**10**	**14**	**18**
empirical	$C_{62.8}H_{63.6}B$-	$C_{66.2}H_{67.5}B$-	$C_{64}H_{67}B$-	$C_{53}H_{42}B$-	$C_{53}H_{43}B$-	$C_{54}H_{45}B$-	$C_{79}H_{66}B$-	$C_{156}H_{137}B_2$-	$C_{56}H_{49}B$-
formula	$Cl_{1.6}F_{24}P_2Rh$	$F_{24.7}InP_2$	$F_{24}NP_2Rh$	$F_{25}PRh$	$F_{24}PRh$	$F_{24}PRh$	$F_{25}P_3Rh$	$F_{49}N_2P_6Rh_2$	$F_{24}PRh$
M_r	1506.72	1597.37	1481.85	1298.56	1280.56	1294.59	1697.95	3383.94	1322.64
space group	monoclinic	orthorhombic	monoclinic	monoclinic	monoclinic	monoclinic	monoclinic	triclinic	monoclinic
	$P2_1/c$	$P2_1cn$	$C2/c$	$C2/c$	$C2/c$	$C2/c$	$P2_1/c$	$P\bar{1}$	$C2/c$
size [mm^3]	0.20×0.15×0.10	0.23×0.15×0.15	0.50×0.33×0.28	0.25×0.25×0.23	0.45×0.45×0.43	0.40×0.40×0.35	0.40×0.40×0.48	0.18×0.15×0.05	0.45×0.23×0.23
a [Å]	20.9755(2)	12.3928(1)	18.5296(2)	19.5546(1)	19.5367(1)	20.2226(1)	23.8394(2)	13.1088(1)	19.9568(1)
b [Å]	12.4126(1)	21.0426(1)	17.4243(2)	16.3567(1)	16.4391(1)	16.3919(1)	13.1178(1)	13.8424(1)	16.4433(1)
c [Å]	25.2091(3)	25.0380(2)	41.7491(5)	34.5797(2)	34.2824(2)	34.1478(2)	26.0538(2)	43.3072(4)	34.9763(3)
α [°]	90	90	90	90	90	90	90	97.2149(3)	90
β [°]	101.413(1)	90	98.8771(4)	106.3826(3)	106.5315(3)	107.1853(4)	113.0628(3)	97.8414(3)	104.847(1)
γ [°]	90	90	90	90	90	90	90	90.0690(3)	90
V [Å^3]	6433.67(11)	6529.33(8)	13317.9(3)	10611.22(11)	10555.20(11)	10814.17(11)	7496.37(10)	7721.95(11)	11094.47(13)
μ [mm^{-1}]	0.487	2.206	0.411	0.477	0.476	0.465	0.398	0.386	0.456
$2\theta_{max}$ [°]	50	52	57.4	59	63	58	60	51	55
N_{obs}	75486	95289	32406	94862	147742	74898	127183	87805	77090
$N_{unique}/R_{(int)}$	11275/	12786/	13162/	14840/	17437/	14383/	21803/	27516/	12661/
	0.0714	0.0585	0.0304	0.0633	0.0475	0.0451	0.0666	0.1043	0.048
N_{param}	1033	945	1073	891	956	920	1154	2093	948
wR_2	0.1259	0.1051	0.1098	0.0938	0.0941	0.1307	0.1152	0.1487	0.1047
(all data)									
R_1 [$I > 2\sigma(I)$]	0.0616	0.0461	0.0520	0.0428	0.0365	0.0484	0.0416	0.0752	0.0421

nbd CH), 37.5 (m, CH), 30.5 (s, CH_2), 25.0 ppm (s, CH_2); elemental analysis calcd (%) for $C_{69}H_{74}BF_{24}P_2Rh{\cdot}0.75\,CH_2Cl_2$: C 52.40, H 4.76; found: C 52.37, H 4.47.

***cis*-[{P(C_5H_7)Cyp$_2$}$_2$Rh][BAr$^F_4$] (2a) and *trans*-[{P(C_5H_7)Cyp$_2$}$_2$Rh]-[BAr$^F_4$] (2b)**: The preparation method used for both complexes **2a** and **2b** was the same with the exception of the timescale employed. An NMR tube was charged with **1** (10 mg, 0.0065 mmol) and CD_2Cl_2 was added via cannula. The solution of complex **1** was left for 2 h (ca. 70% of **2a)**, and characterisation was achieved by NMR spectroscopy. For complex **2b**, the solution was left for two days (ca. 70% of **2b**), and characterisation was achieved by NMR spectroscopy.

Yellow/orange crystals of complex **2b** were grown after 2 d by diffusion of pentane into a concentrated solution of the complex in CH_2Cl_2. The resulting crystals contained a mixture of products; however a single crystal suitable for X-ray diffraction could be selected. Crystals of the mixed species **2a·2b** were grown by similar means except that the diffusion of pentane into a concentrated solution of the complex in CH_2Cl_2 was carried out after 2 h.

NMR data for complex **2a**: selected ^{1}H NMR (400.1 MHz, CD_2Cl_2): δ = 4.90 ppm (s); ^{31}P{^{1}H} (161.9 MHz, CD_2Cl_2): δ = 67.35 ppm [d, J(P,Rh) = 150 Hz]; selected ^{13}C{^{1}H} (100.6 MHz, CD_2Cl_2): δ = 100.94 [m, J(P,P) = 50, J(P^1,C) = 8.7, J(Rh,C) = 8.1, J(P^2,C) = 3.0 Hz].

NMR data for complex **2b**: selected ^{1}H NMR (400.1 MHz, CD_2Cl_2): δ = 5.46 ppm (s); ^{31}P{^{1}H} (161.9 MHz, CD_2Cl_2): δ = 65.79 [d, J(P,Rh) = 114 Hz]; selected ^{13}C{^{1}H} (100.6 MHz, CD_2Cl_2): δ = 89.2 ppm [d, J-(Rh,C) = 10.2 Hz]; elemental analysis calcd (%) for $C_{62}H_{62}BF_{24}P_2Rh$: C 51.76, H 4.34; found: C 51.62, H 4.52; ESI-MS (CH_2Cl_2): m/z: calcd for $[RhP_2C_{30}H_{50}]^+$: 575.2437; found 575.2444.

[Ir{PCyp$_2$(η^2-C_5H_7)}$_2$H$_2$][BAr$^F_4$] (4): A hexane solution of PCyp$_3$ (0.22 mL, 0.49 M, 0.11 mmol) was added to a solution of [Ir(coe)$_2$Cl]$_2$ (25 mg, 2.29×10^{-2} mmol) in CH_2Cl_2 (5 mL). The mixture was stirred overnight. The solvent was removed in vacuo and the residue redissolved in pentane and stored at −78 °C to yield a yellow powder. The solid was isolated and dissolved in CH_2Cl_2 (5 mL) and to it Na[BAr$^F_4$] (49 mg, 5.58×10^{-2} mmol) and 3,3-dimethyl-1-butene (35 μL, 0.279 mmol) were added. The mixture was filtered and the solvent removed in vacuo. Colourless, X-ray quality, crystals were obtained by diffusion of pentane into a solution of the complex in C_6H_5F. (24 mg, 34%). ^{1}H NMR (400.11 MHz, CD_2Cl_2): δ = 7.72 (s, 8H, BAr$^F_4$), 7.55 (s, 4H, BAr$^F_4$), 4.69 (m, 2H, η^2-HC=CH), 4.50 (m, 2H, η^2-HC=CH), 2.4–1.4 (m, 46H, CH/CH_2), −12.17 ppm [t, J(P,H) = 11.4 Hz, 2H, IrH]; ^{31}P{^{1}H} NMR (162.0 MHz, CD_2Cl_2): δ = 39.5 ppm (s); elemental analysis calcd (%) for $IrC_{62}H_{64}P_2BF_{24}{\cdot}0.7\,(C_6H_5F)$: C 49.78, H 4.26; found: C 49.52, H 4.26; ESI-MS (CH_2Cl_2): m/z: calcd for $[^{193}IrC_{30}H_{52}P_2]^+$: 667.3169; found: 667.3165.

[(PCyp$_3$)$_2$Rh(H)$_2$(η^2-H$_2$)$_2$][BAr$^F_4$] (5): A NMR tube was charged with complex **1** (10 mg, 0.0065 mmol) and CD_2Cl_2 (0.5 mL) was transferred via cannula into the tube. The tube was frozen in liquid N_2, placed under vacuum and backfilled with H_2. Upon thawing, the solution rapidly changed from yellow to colourless. The solution was characterised by NMR. Complex **5** is only stable under a H_2 atmosphere and thus no microanalysis was obtained. ESI-MS shows $[M-(2\times H_2)]^+$ consistent with the weak binding of two dihydrogen ligands. ^{1}H NMR (400.1 MHz, CD_2Cl_2, 200 K): δ = 7.9 (s, 8H, BAr$^F_4$), 7.75 (s, 4H, BAr$^F_4$), 1–2.3 (m, 54H, 2(C_5H_9)$_3$), −2.21 (brs, 4H, T_1 = 14 ms, RhH$_2$), −13.79 ppm (brs, 2H, T_1 = 250 ms, Rh-H); ^{31}P{^{1}H} NMR (161.9 MHz, CD_2Cl_2): δ = 57.43 ppm [d, J(Rh,P) = 101 Hz].

[{P(η^2-C_5H_7)Cyp$_2$}{PCyp$_3$}Rh(MeCN)][BAr$^F_4$] (6): A solution of **1** (40 mg, 0.026 mmol) in C_6H_5F (5 mL) in a J. Young's tube was placed under 4 atm hydrogen and shaken for 5 min. The solution was freeze-thaw-degassed to remove excess hydrogen and 3,3-dimethylbutene (100 μL) was added at 77 K. The mixture was allowed to thaw and mixed for several seconds. MeCN (100 μL) was added via cannula, the mixture was shaken and the solution was layered with cyclohexane. After 3 d the mixture was filtered to give **6** as yellow-orange crystals (20 mg, 53%). A single crystal suitable for X-ray crystallography was grown by diffusion of pentane into a concentrated solution of the complex in CH_2Cl_2. ^{1}H NMR (400.1 MHz, CD_2Cl_2): δ = 7.72 (s, 8H, BAr$^F_4$), 7.55 (s, 4H, BAr$^F_4$), 4.25 (s, 2H, CH=CH), 2.32 (s, 3H, NCCH$_3$), 1.28–2.2 ppm (m, 50H, (C_5H_9)$_5$-(C_5H_7)); ^{31}P{^{1}H} NMR (161.9 MHz, CD_2Cl_2): δ = 74.58 [dd, J(P,P) = 302, J(Rh,P) = 123 Hz], 25.67 [dd, J(P,P) = 302, J(Rh,P) = 117 Hz]; ^{13}C{^{1}H} NMR (100.6 MHz, CD_2Cl_2): δ = 162.1 [q, J(B,C) = 50 Hz, BAr$^F_4$], 135.1 (s, BAr$^F_4$), 129.2 [qq, J(F,C) = 31, J(B,C) = 2.9 Hz, BAr$^F_4$], 128.99 (s, C≡N), 124.94 (q, J(F,C) = 272 Hz, BAr$^F_4$), 117.78 (s, BAr$^F_4$), 71.0 [d, J(Rh,C) = 15 Hz, HC=CH], 37.94 [dd, J(P,C) = 7.8, J-(Rh,C) = 2.1 Hz, CH_2], 35.45 [dd, J(P,C) = 18, J(Rh,C) = 1.8 Hz, CH], 33.27 [dd, J(P,C) = 20, J(Rh,C) = 1.9 Hz, CH], 31.94 (s, CH_2), 30.61 [d, J(P,C) = 2.8 Hz, CH_2], 29.9 (s, CH_2), 27.04 [dt, J(P,C) = 24, J(Rh,C) ≈ J-(P,C) ≈ 2.2 Hz, CH], 26.86 [d, J(P,C) = 7.9 Hz, CH_2], 26.35 [d, J(P,C) = 8.1 Hz, CH_2], 26.2 (d, J(P,C) = 8.8 Hz, CH_2); elemental analysis calcd (%) for $C_{64}H_{67}BF_{24}N_1P_2Rh$: C 51.87, H 4.56, N 0.95; found: C 51.79, H 4.65, N 0.93; ESI-MS (CH_2Cl_2): m/z: calcd for $[RhP_2C_{32}H_{55}N]^+$: 618.2859; found: 618.2850.

[Rh(η^6-C_6H_5F){PCyp$_2$(η^2-C_5H_7)}][BAr$^F_4$] (7): A mixture Rh(nbd)-(PCyp$_3$)Cl (50.0 mg, 0.11 mmol) and Na[BAr$^F_4$] (94.75 mg, 0.11 mmol) in C_6H_5F (5 mL) was stirred for 1 h. The mixture was filtered and the solution was layered with pentane. Slow diffusion gave **7** as pale yellow crystals (84 mg, 61%). ^{1}H NMR (400.11 MHz, C_6H_5F): δ = 8.29 (s, 8H, BAr$^F_4$), 7.63 (s, 4H, BAr$^F_4$), 6.07 (m, 4H, ArH), 5.45 (m, 1H, *p*ArH), 3.89 (d, J = 3.0 Hz, 2H, HC=CH), 1.70–1.05 ppm (m, 23H, CH/CH_2); ^{31}P{^{1}H} NMR (162.0 MHz, C_6H_5F): δ = 109.67 [dd, J(Rh,P) = 178, J-(F,P) = 3.9 Hz]; selected ^{13}C{^{1}H} NMR (100.6, C_6H_5F): δ = 145.55 [dt, J-(F,C) = 275, J = 2.6 Hz, C_5H_5CF], 103.32 [ddd, J(F,C) = 7.1, J = 2.7, 1.5 Hz, C_6H_5F], 96.30 (ddd, J = 3.7, 2.7, 1.1 Hz, C_6H_5F), 92.23 [dt, J(F,C) = 20, 2.0 Hz, C_6H_5F], 65.04 [d, J(Rh,C) = 16 Hz, HC=CH], 36.15 [d, J-(P,C) = 3.7 Hz, CH_2], 35.20 [dd, J(P,C) = 26, J(Rh,C) = 1.1 Hz, CH], 32.22 (s, CH_2), 30.08 [dd, J(P,C) = 29, J(Rh,C) = 2.2 Hz, CH], 30.06 (s, CH_2), 27.23 [d, J(P,C) = 8.4 Hz, CH_2], 26.32 ppm [d, J(P,C) = 9.3 Hz, CH_2]; elemental analysis calcd (%) for $C_{53}H_{42}BF_{25}PRh$: C 49.02, H 3.26; found: C 49.41, H 3.29.

[Rh(η^6-C_6H_6){PCyp$_2$(η^2-C_5H_7)}][BAr$^F_4$] (8): A mixture of benzene (0.2 mL, 2.9×10^{-3} mol), [Rh(nbd)(PCyp$_3$)Cl] (20.0 mg, 4.2×10^{-2} mmol) and Na[BAr$^F_4$] (37.9 mg, 4.2×10^{-2} mmol) in CH_2Cl_2 (5 mL) was stirred for 1 h. The mixture was filtered and the solvent was removed in vacuo. Diffusion of pentane into a solution of the residue in CH_2Cl_2 gave **8** as pale yellow crystals (28 mg, 52%). ^{1}H NMR (400.1 MHz, CD_2Cl_2): δ = 7.70 (s, 8H, BAr$^F_4$), 7.55 (s, 4H, BAr$^F_4$), 6.55 (s, 6H, C_6H_6), 4.30 (d, J = 2.7 Hz, 2H, HC=CH), 2.15–1.35 ppm (m, 23H, CH/CH_2); ^{31}P{^{1}H} NMR (162.0 MHz, CD_2Cl_2): δ = 111.45 ppm [d, J(Rh,P) = 178 Hz]; ^{13}C{^{1}H} NMR (100.6, CD_2Cl_2): δ = 162.10 [q, J(B,C) = 50 Hz, BAr$^F_4$], 135.14 (s, BAr$^F_4$), 129.21 [qq, J(F,C) = 31, J(B,C) = 2.9 Hz, BAr$^F_4$], 124.94 [q, J-(F,C) = 272 Hz, BAr$^F_4$], 117.81 (s, BAr$^F_4$), 102.53 (s, C_6H_6), 62.72 [d, J-(Rh,C) = 16 Hz, HC=CH], 36.44 [d, J(P,C) = 4.0 Hz, CH_2], 35.33 [d, J-(P,C) = 26 Hz, PCH], 32.55 (s, CH_2), 30.33 (s, CH_2), 30.15 [dd, J(P,C) = 28, J(Rh,C) = 2.2 Hz, PCH], 27.10 [d, J(P,C) = 8.8 Hz, CH_2], 26.32 [d, J-(P,C) = 9.5 Hz, CH_2]: elemental analysis calcd (%) for $C_{53}H_{43}BF_{24}PRh$: C 49.71, H 3.38; found: C 49.58, H 3.34.

[Rh(nbd){PCyp$_2$(η^2-C_5H_7)}][BAr$^F_4$] (9): Norbornadiene (0.1 mL, 1.0 mmol) was added to a solution of **7** (30 mg, 0.023 mmol) in CH_2Cl_2 (2 mL) and the resulting solution was stirred for 1 h. The solvent was removed *in vacuo*, the residue was dissolved in CH_2Cl_2 and the solution was layered with pentane to give **9** as yellow crystals (24 mg, 80%). ^{1}H NMR (400.1 MHz, C_6H_5F): δ = 7.71 (s, 8H, BAr$^F_4$), 7.55 (s, 4H, BAr$^F_4$), 5.83 (m, 2H, nbd CH), 5.46 (d, J = 2.0 Hz, 2H, C_5H_7 HC=CH), 5.39 (m, 2H, nbd HC=CH), 4.16 (m, 2H, nbd HC=CH), 2.44–1.40 ppm (m, 23H, CH/CH_2); ^{31}P{^{1}H} NMR (162.0 MHz, C_6H_5F): δ = 73.08 [d, J-(Rh,P) = 151 Hz]; ^{13}C{^{1}H} NMR (125.8 MHz, CD_2Cl_2): δ = 162.14 [q, J-(B,C) = 50 Hz, BAr$^F_4$], 135.17 (s, BAr$^F_4$), 129.24 [qq, J(F,C) = 31, J(B,C) = 2.9 Hz, BAr$^F_4$], 124.91 [q, J(F,C) = 273 Hz, BAr$^F_4$], 117.84 (s, BAr$^F_4$), 108.99 [d, J(Rh,C) = 9.1 Hz, C_5H_7 HC=CH], 95.78 (dd, J = 9.1, 5.4 Hz, nbd HC=CH), 86.22 [d, J(Rh,C) = 8.2 Hz, nbd HC=CH], 71.51 (m, nbd CH_2), 56.29 (m, nbd CH), 38.39 [d, J(Rh,C) = 5.4 Hz, CH_2], 33.28 [d, J-(Rh,C) = 23 Hz, CH], 31.24 (s, CH_2), 30.54 [d, J(Rh,C) = 24 Hz, CH], 29.79 (s, CH_2), 26.89 [d, J(Rh,C) = 8.2 Hz, CH_2], 26.19 [d, J(Rh,C) = 8.2 Hz, CH_2; signals were assigned using 2D COSY and NOESY experi-

ments; elemental analysis calcd (%) for $C_{54}H_{45}BF_{24}PRh$: C 50.1, H 3.50; found: C 49.38, H 3.48.

[Rh(dppe){PCyp$_2$(η^2-C$_5$H$_7$)}][BAr$^F_4$] (10): A mixture of Rh(dppe)(PCyp$_3$)Cl (30 mg, 3.87×10^{-2} mmol) and Na[BAr$^F_4$] (34 mg, 0.0387 mmol) in CH_2Cl_2 (5 mL) was stirred for 15 minutes. The resulting orange mixture was filtered and the solvent was removed in vacuo. Diffusion of pentane into a solution of the residue in C_6H_5F gave **10** as orange crystals (38 mg, 61%). ^{1}H NMR (400.11 MHz, CD_2Cl_2): δ = 7.72 (m, 8H, BAr$^F_4$), 7.55 (s, 4H, BAr$^F_4$), 7.70–7.45 (m, 20H, ArH), 4.89 (m, 2H, HC=CH), 2.2–1.2 ppm (m, 27H, CH/CH$_2$); ^{31}P{^{1}H} NMR (162.0 MHz, CD_2Cl_2): δ = 65.03 [ddd, J(P,P) = 283, J(Rh,P) = 125, J(P,P) = 31 Hz, PCyp], 60.55 [ddd, J(P,P) = 283, J(Rh,P) = 125, J(P,P) = 28 Hz, P$_{DPPE}$ *trans* to PCyp], 50.53 ppm [ddd, J(Rh,P) = 158, J(P,P) = 31, J(P,P) = 28 Hz, P$_{DPPE}$ *trans* to alkene]; signals assigned using 2D ^{31}P HMQC and NOESY experiments; ^{13}C{^{1}H} NMR (100.6, CD_2Cl_2): δ = 162.10 [q, J-(B,C) = 50 Hz, BAr$^F_4$], 135.14 (s, BAr$^F_4$), 133.44 [d, J(P,C) = 12 Hz, Ar CH], 133.24 [d, J(P,C) = 11 Hz, Ar CH], 133.23 [d, J(P,C) = 41 Hz, Ar CH], 131.87 [d, J(P,C) = 11 Hz, Ar CH], 131.85 [d, J(P,C) = 11 Hz, Ar CH], 131.33 [dd, J(P,C) = 37, J(Rh,C) = 3.5 Hz, Ar CH], 129.71 [d, J-(P,C) = 9.3 Hz, Ar CH], 129.46 [d, J(P,C) = 10 Hz, Ar CH], 129.2 [q, J-(F,C) = 31 Hz, BAr$^F_4$], 124.94 [q, J(F,C) = 272 Hz, BAr$^F_4$], 117.79 (s, BAr$^F_4$), 96.21 (t, J = 9.7 Hz, HC=CH), 37.75 [d, J(P,C) = 7.5 Hz, CH$_2$], 35.52 [d, J(P,C) = 19 Hz, CH], 31.27 (s, CH$_2$), 29.91 (s, CH$_2$), 29.48 [dd, J(P,C) = 19, J(Rh,C) = 3.3 Hz, CH], 26.43 [d, J(P,C) = 7.9 Hz, CH$_2$], 25.60 ppm [d, J(P,C) = 8.4 Hz, CH$_2$]; elemental analysis calcd (%) for $C_{71}H_{61}BF_{24}P_3Rh$: C 54.77, H 3.84; found: C 54.73, H 3.78.

[(dppe)(PCyp$_3$)Rh(η^2-H$_2$)(H)$_2$][BAr$^F_4$] (11): A solution of **10** (10 mg, 6.26×10^{-3} mmol) in CD_2Cl_2 was placed under 4 atm of H_2 (298:77 = 3.8) and shaken for 15 min. The product was characterized in situ by ^{1}H, ^{13}C{^{1}H} and ^{31}P{^{1}H} NMR spectroscopy. Compound **11** loses H_2 when removed from a H_2 atmosphere and thus microanalytical data was not obtained. ^{1}H NMR (400.1 MHz, CD_2Cl_2, 298 K): δ = 7.72 (s, 8H, BAr$^F_4$), 7.59–7.42 (m, 20H, ArH), 7.54 (s, 4H, BAr$^F_4$), 2.46 (m, 4H, dppe CH$_2$), 1.91 (apparent quintet, J = 8.9 Hz, 3H, CH), 1.81–1.18 (m, 24H, CH$_2$), −4.5 (v brs, fwhm 1800 Hz, ≈2.5H); ^{31}P{^{1}H} NMR (162.0 MHz, CD_2Cl_2, 298 K): δ = 56.98 ppm (br m); ^{1}H NMR (400.1 MHz, CD_2Cl_2, 180 K): δ = 7.83–6.98 (m, 20H, ArH), 7.72 (s, 8H, BAr$^F_4$), 7.51 (s, 4H, BAr$^F_4$), 3.01–0.94 (m, 31H, CH$_2$/CH), −3.12 (s, 2H, T_1 = 19 ms, RhH$_2$), −8.51 [ddt, J(P$_{trans}$,H) = 149, J = 14, 8.5 Hz, 1H, T_1 = 215 ms, RhH], −13.03 (m, 1H, T_1 = 250 ms, RhH); ^{31}P{^{1}H} NMR (202.5 MHz, CD_2Cl_2, 220 K): δ = 61.35 [ddd, J(P,P) = 285, J(Rh,P) = 99, J(P,P) = 12 Hz], 59.63 [ddd, J(P,P) = 285, J(Rh,P) = 98, J(P,P) = 15 Hz], 51.83 ppm [ddd, J(Rh,P) = 86, J(P,P) = 15, J(P,P) = 12 Hz]; selected ^{13}C{^{1}H} NMR (125.8 MHz, CD_2Cl_2, 200 K): δ = 36.15 (m, P-CH), 29.54 (s, CH$_2$), 29.14 (s, CH$_2$), 25.33 (s, CH$_2$)*; no signals between δ 60 and 110 ppm. The signal marked * has a high intensity suggesting two coincident signals.

[(dppe)Rh(PCyp$_3$)(L)(H)$_2$][BAr$^F_4$] (12) (L = solvent or agostic interaction): A solution of **10** (5 mg, 3.13×10^{-3} mmol) in CD_2Cl_2 was placed under 4 atm of H_2 (298:77 = 3.8) and shaken for 15 min to give **11**. The H_2 was removed under vacuum by freeze/pump/thaw of the solution and the product was immediately characterized in situ by ^{1}H and ^{31}P{^{1}H} NMR spectroscopy at 180 K. ^{1}H NMR (500.1 MHz, CD_2Cl_2, 180 K): δ = 7.71 (s, 8H, BAr$^F_4$), 7.51 (s, 4H, BAr$^F_4$), 7.48–7.20 (m, 20H, ArH), 3.19–0.46 (m, 31H, CH/CH$_2$), −8.39 (br s, 1H, Rh-H), −20.51 ppm (br s, 1H, Rh-H); ^{1}H NMR (500.1 MHz, CD_2Cl_2, 250 K): δ = 7.70 (s, 8H, BAr$^F_4$), 7.62–7.23 (m, 20H, ArH), 7.52 (s, 4H, BAr$^F_4$), 2.89–0.88 (m, 31H, CH/CH$_2$), −14.59 ppm (br s, 2H, Rh-H); ^{31}P{^{1}H} NMR (202.5 MHz, CD_2Cl_2, 180 K): δ = 61.85 [ddd, J(P,P) = 314, J(Rh,P) = 101, J(P,P) = 11 Hz], 51.84 [br dd, J(P,P) = 314, J(Rh,P) = 101 Hz], 46.41 [dt, J(Rh,P) = 87, J(P,P) = 11 Hz].

[(dppe)(PCyp$_3$)Rh(MeCN)(H)$_2$][BAr$^F_4$] (13): A solution of **10** (5 mg, 3.13×10^{-3} mmol) in CD_2Cl_2 was placed under 4 atm of H_2 (298:77 = 3.8) and shaken for 15 minutes to give **11**. MeCN (50 μL) was added and the solution again placed under 4 atm of H_2 to avoid loss of H_2. The product was immediately characterized in situ by ^{1}H and ^{31}P{^{1}H} NMR spectroscopy at 200 K. ^{1}H NMR (500.1 MHz, CD_2Cl_2, 200 K): δ = 7.70 (s, 8H, BAr$^F_4$), 7.51 (s, 4H, BAr$^F_4$), 7.49–7.20 (m, 20H, ArH), 2.76–0.97 (m, 31H, CH$_2$/CH), −8.94 [dt, J(P,H) = 160, J(Rh/P,H) = 14 Hz, 1H, RhH], −17.99 ppm (m, 1H, RhH); excess MeCN present so coordinated MeCN not unequivocally observed; ^{31}P{^{1}H} NMR (202.5 MHz, CD_2Cl_2, 200 K): δ = 66.82 [ddd, J(P,P) = 319, J(Rh,P) = 101, J(P,P) = 11 Hz, P$_{DPPE}$ *trans* to PCyp$_3$], 54.84 [ddd, J(P,P) = 319, J(Rh,P) = 106, J(P,P) = 18 Hz, PCyp$_3$], 45.92 [ddd, J(Rh,P) = 87, J(P,P) = 18, J(P,P) = 11 Hz, P$_{DPPE}$ *trans* to H]; signals assigned using 2D HMQC experiments.

[(dppe)Rh(PCyp$_3$)(MeCN)][BAr$^F_4$] (14): A solution of **10** (10 mg, 6.26×10^{-3} mmol) in CH_2Cl_2 (2 mL) and MeCN (0.1 mL) was placed under 4 atm of H_2 (298:77 = 3.8) and the solution was stirred for 2 h. The solvent was removed in vacuo and the resulting yellow oil was washed with pentane (2×2 mL). The residue was recrystallised by diffusion of pentane into a solution of the complex in C_6H_5F to give **14** as pale yellow crystals (6 mg, 58%). ^{1}H NMR (500.1 MHz, CD_2Cl_2, 298 K): δ = 7.83 (m, 4H, ArH), 7.67 (m, 4H, ArH), 7.68 (s, 8H, BAr$^F_4$), 7.57–7.41 (m, 12H, ArH), 7.54 (s, 4H, BAr$^F_4$), 2.15 [dq, ^2J(P,H) = 31, ^3J(P,H) ≈ J(H,H) = 7.1 Hz, 2H, P-CH$_2$], 1.87 [dq, ^2J(P,H) = 26, ^3J(P,H) ≈ J(H,H) = 7.1 Hz, 2H, P-CH$_2$], 1.79–1.15 (m, 27H, CH$_2$/CH), 1.68 ppm (s, 3H, NCCH$_3$); ^{31}P{^{1}H} NMR (202.5 MHz, CD_2Cl_2, 298 K): δ = 66.06 [dt, J(Rh,P) = 181, J(P,P) = 35 Hz, P$_{DPPE}$ *trans* to MeCN], 62.27 [ddd, J(P,P) = 282, J(Rh,P) = 128, J(P,P) = 35 Hz, P$_{DPPE}$ *trans* to PCyp$_3$], 27.80 [ddd, J(P,P) = 282, J-(Rh,P) = 127, J(P,P) = 35 Hz, PCyp$_3$]; signals assigned using 2D HMQC experiments; ^{13}C{^{1}H} NMR (125.8 MHz, CD_2Cl_2): δ = 162.10 [q, J(B,C) = 50 Hz, BAr$^F_4$], 135.17 (s, BAr$^F_4$), 134.11 [d, J(P,C) = 10.9 Hz, Ar CH], 133.50 [d, J(P,C) = 10.9 Hz, Ar CH], 133.30 [d, J(P,C) = 40 Hz, Ar PC], 132.50 [d, J(P,C) = 40 Hz, Ar PC], 131.50 [d, J(P,C) = 2.0 Hz, Ar CH], 131.33 [dd, J(P,C) = 2.0 Hz, Ar CH], 130.39 [d, J(Rh,C) = 7.3 Hz, N≡C], 129.23 [qq, J(F,C) = 32, J(B,C) = 2.7 Hz, BAr$^F_4$], 129.31 [d, J(P,C) = 9.1 Hz, Ar CH], 128.9 [d, J(P,C) = 9.1 Hz, Ar CH], 124.94 [q, J(F,C) = 272 Hz, BAr$^F_4$], 117.79 [sept, J(F,C) = 3.6 Hz, BAr$^F_4$], 36.76 [d, J(P,C) = 21 Hz, CH], 34.11 (m, P-CH$_2$), 30.78 [d, J(P,C) = 1.8 Hz, CH$_2$], 26.01 [d, J(P,C) = 9 Hz, CH$_2$], 24.25 (m, P-CH$_2$), 3.49 ppm (s, *C*H$_3$CN); ESI-MS (C_6H_5F): m/z: calcd for $[C_{43}H_{54}NP_3Rh]^+$: 780.25; found: 780.30.

[Rh(dppe)P(C$_6$H$_{11}$)$_3$(L)][BAr$^F_4$] (L = solvent or agostic interaction) (15): Na[BAr$^F_4$] (21.7 mg, 0.024 mmol) was added to a solution of [Rh(dppe)(PCy$_3$)Cl] in CH_2Cl_2 (1 mL), the resulting mixture was stirred for 5 minutes and the product was characterised in situ by ^{1}H and ^{31}P{^{1}H} NMR spectroscopy and ESI-MS. ^{1}H NMR (500.1 MHz, CD_2Cl_2, 298 K): δ = 7.75–7.67 (m, 4H, ArH), 7.71 (s, 8H, BAr$^F_4$), 7.57–7.46 (m, 16H, ArH), 7.54 (s, 4H, BAr$^F_4$), 2.20–1.01 ppm (m, 37H, CH/CH$_2$); ^{31}P{^{1}H} NMR (202.5 MHz, CD_2Cl_2, 298 K): δ = 68 (br s), 22 (vbr s); ^{1}H NMR (500.13 MHz, CD_2Cl_2, 190 K): δ = 7.96–7.02 (m, 12H, ArH), 7.71 (s, 8H, BAr$^F_4$), 7.51 (s, 4H, BAr$^F_4$), 3.06–0.08 ppm (m, 37H, CH/CH$_2$); ^{31}P{^{1}H} NMR (202.5 MHz, CD_2Cl_2, 180 K): shows many resonances (δ 80–20) consistent with a mixture of products; ESI-MS (C_6H_5F): m/z: calcd for $[C_{44}H_{57}P_3Rh]^+$: 781.272; found: 781.277.

[Rh(dppe)(PCy$_3$)(MeCN)][BAr$^F_4$] (16): Na[BAr$^F_4$] (21.7 mg, 0.024 mmol) was added to a solution of Rh(dppe)(PCy$_3$)Cl in CH_2Cl_2 (1 mL) and the resulting mixture was stirred for 5 minutes. MeCN (0.1 mL) was added to the mixture and the product was characterised in situ by ^{1}H and ^{31}P{^{1}H} NMR spectroscopy and ESI-MS. ^{1}H NMR (500.11 MHz, CD_2Cl_2): δ = 7.84 (m, ArH), 7.71 (m, ArH), 7.69 (s, 8H, BAr$^F_4$), 7.54 (s, 4H, BAr$^F_4$), 7.52–7.41 (m, ArH), 2.26–0.78 ppm (m, 40H, CH/CH$_2$); excess MeCN present so coordinated MeCN not unequivocally observed; ^{31}P{^{1}H} NMR (202.5 MHz, CD_2Cl_2): δ = 66.13 [ddd, J(Rh,P) = 182, J(P,P) = 35, J-(P,P) = 35 Hz, P$_{dppe}$ *trans* to MeCN], 63.19 [ddd, J(P,P) = 277, J(Rh,P) = 128, J(P,P) = 35 Hz, P$_{dppe}$ *trans* to PCy$_3$], 30.36 ppm [ddd, J(P,P) = 277, J(Rh,P) = 125, J(P,P) = 35 Hz, PCy$_3$]. Signals assigned using 2D HMQC experiments; ESI-MS (C_6H_5F): m/z: calcd for $[C_{46}H_{60}NP_3Rh]^+$: 822.2988; found: 822.2982.

[Rh(η^6-C$_6$H$_5$F){P(η^2-C$_5$H$_7$)(Cy)$_2$][BAr$^F_4$] (17): Na[BAr$^F_4$] (69.2 mg, 0.0781 mmol) was added to a solution of [Rh(nbd)Cl{PCy$_2$Cyp}] (38.9 mg, 0.0783 mmol) in C_6H_5F (≈2 mL) and the resulting mixture was stirred for 18 h. The mixture was filtered and the solvent removed in vacuo to give a yellow residue that was then washed with pentane to give **17** as a yellow powder (Crude yield, 71.3 mg, 68%). Attempting to purify the complex further lead to decomposition. ^{1}H NMR (400.1 MHz, C_6H_5F): δ = 8.30 (s, 8H, BAr$^F_4$), 7.62 (s, 4H, BAr$^F_4$), 6.03–6.11 (m, 3H,

C_6H_5F), 5.51 (m, 2H, C_6H_5F), 3.89 (br d, 2H, HC=CH), 0.8–2.2 ppm (m, 29H, $2C_6H_{11}$, $2CH_2$ and CH of C_5H_7); $^{31}P\{^1H\}$ NMR (162.0 MHz, C_6H_5F): δ = 112.23 ppm [dd, J(Rh,P) = 180, J(F,P) = 3.1 Hz]; selected $^{13}C\{^1H\}$ NMR (125.8 MHz, C_6H_5F): δ = 102.84 (m, C_6H_5F), 96.09 (m, C_6H_5F), 91.97 [d, J(F,C) = 20 Hz, C_6H_5F], 65.03 [d, J(Rh,C) = 16 Hz, C=C].

$[Rh(\eta^6\text{-}C_6H_5Me)\{PCy_2(\eta^2\text{-}C_5H_7)\}][BAr^F{}_4]$ (18): $Na[BAr^F{}_4]$ (66.2 mg, 0.0747 mmol) was added to a solution of [Rh(nbd)Cl{PCy_2Cyp}] (36.8 mg, 0.0741 mmol) in C_6H_5F ($\approx$2 mL) and the resulting mixture was stirred for 18 h. Toluene ($\approx$0.3 mL) was added and the mixture was stirred for a further hour and filtered. Diffusion of pentane into a solution of the complex in C_6H_5F gave **18** as pale yellow crystals (60.2 mg, 61%). ^1H NMR (500.1 MHz, CD_2Cl_2): δ = 7.7 (s, 8H, $BAr^F{}_4$), 7.5 (s, 4H, $BAr^F{}_4$), 6.6 (m, 3H, $C_6H_5CH_3$), 6.3 (d, 2H, $C_6H_5CH_3$), 4.1 (br d, 2H, HC=CH), 2.3 (s, 3H, $C_6H_5CH_3$), 1.1–2.5 ppm (m, 29H, $2C_6H_{11}$, C_5H_7); $^{31}P\{^1H\}$ NMR (202.5 MHz, CD_2Cl_2): δ = 111.83 [d, J(Rh,P) = 180 Hz]; $^{13}C\{^1H\}$ NMR (125.8 MHz, CD_2Cl_2): δ = 162.06 [q, J(B,C) = 50 Hz, $BAr^F{}_4$], 135.10 (s, $BAr^F{}_4$), 129.17 [qq, ^1J(F,C) = 32, ^2J(F,C) = 3.0 Hz, $BAr^F{}_4$], 124.91 [q, ^1J(F,C) = 272 Hz, $BAr^F{}_4$], 119.58 [dd, J(Rh,C) = 4.3 Hz, J(P,C) = 2.0 Hz, ipso-$C_6H_5CH_3$), 117.77 (m, $BAr^F{}_4$), 103.20 [dd, J(Rh,C) = 3.6, J(P,C) = 2.5 Hz, $C_6H_5CH_3$], 101.96 [dd, J(Rh,C) = 2.8, J(P,C) = 0.96 Hz, $C_6H_5CH_3$], 99.40 [d, J(Rh,C) = 2.8 Hz, $C_6H_5CH_3$], 64.30 [d, J(Rh,C) = 16 Hz, C=C], 36.72 [d, J(P,C) = 4.4 Hz, CH_2], 36.36 [dd, J(P,C) = 21 Hz, J(Rh,C) = 1.2 Hz, CH], 31.69 [dd, J(P,C) = 2.8, J(Rh,C) = 1.1 Hz, CH_2], 29.66 [d, J(P,C) = 2.1 Hz, CH_2], 27.58 [d, J(P,C) = 11 Hz, CH_2], 27.46 [dd, J(P,C) = 27, J(Rh,C) = 1.9 Hz, CH], 27.46 [d, J(P,C) = 11 Hz, CH_2], 25.94 [d, J(P,C) = 1.5 Hz, CH_2], 19.94 (s, $C_6H_5CH_3$); elemental analysis calcd (%) for $C_{56}H_{49}BF_{24}PRh\cdot(C_5H_{12})_{0.5}$: C 51.71, H 4.08; found: C 51.92, H 3.76; ESI-MS (C_6H_5F): m/z: calcd for $[RhPC_{24}H_{37}]^+$: 459.1682; found: 459.1695.

Acknowledgements

The Royal Society (A.S.W.), the Royal Society of Edinburgh (S.A.M.), the ESPRC for funding (A.S.W., S.A.M.) and Heriot-Watt University for a James Watt Bursary (P.V.). Mr. James Kerr for preliminary experiments.

[1] K. I. Goldberg, A. S. Goldman in *Activation and Functionalization of C-H Bonds, Vol. 885* Americam Chemical Society, Washington, **2004**.
[2] J. A. Labinger, J. E. Bercaw, *Nature* **2002**, *417*, 507–514.
[3] R. H. Crabtree, *J. Chem. Soc. Dalton Trans.* **2001**, 2437–2450.
[4] G. J. Kubas, *Metal Dihydrogen and σ-Bond Complexes*, Kluwer Academic/Plenum Publishers, New York, **2001**.
[5] M. J. Burk, R. H. Crabtree, *J. Am. Chem. Soc.* **1987**, *109*, 8025–8032.
[6] A. S. Goldman, A. H. Roy, Z. Huang, R. Ahuja, W. Schinski, M. Brookhart, *Science* **2006**, *312*, 257–261.
[7] K. M. Zhu, P. D. Achord, X. W. Zhang, K. Krogh-Jespersen, A. S. Goldman, *J. Am. Chem. Soc.* **2004**, *126*, 13044–13053.
[8] C. M. Jensen, *Chem. Commun.* **1999**, 2443–2449.
[9] M. A. Bennett, G. B. Robertson, P. O. Whimp, P. W. Clark, *J. Chem. Soc. Chem. Commun.* **1972**, 1011-&.
[10] S. Hietkamp, D. J. Stufkens, K. Vrieze, *J. Organomet. Chem.* **1978**, *152*, 347–357.
[11] D. Amoroso, V. P. A. Yap, D. E. Fogg, *Can. J. Chem.* **2001**, *79*, 958–963.
[12] C. Six, B. Gabor, H. Gorls, R. Mynott, P. Philipps, W. Leitner, *Organometallics* **1999**, *18*, 3316–3326.
[13] S. Sabo-Etienne, B. Chaudret, *Coord. Chem. Rev.* **1998**, *180*, 381–407.
[14] A. F. Borowski, S. SaboEtienne, M. L. Christ, B. Donnadieu, B. Chaudret, *Organometallics* **1996**, *15*, 1427–1434.
[15] M. A. Esteruelas, A. M. Lopez, *Organometallics* **2005**, *24*, 3584–3613.
[16] M. Baya, M. L. Buil, M. A. Esteruelas, E. Onate, *Organometallics* **2004**, *23*, 1416–1423.
[17] E. Piras, F. Läng, H. Rüegger, D. Stein, M. Wörle, H. Grützmacher, *Chem. Eur. J.* **2006**, *12*, 5849–5858.
[18] S. Deblon, L. Liesum, J. Harmer, H. Schönberg, A. Schweiger, H. Grützmacher, *Chem. Eur. J.* **2002**, *8*, 601–611.
[19] W. H. Bernskoetter, E. Lobkovsky, P. J. Chirik, *Organometallics* **2005**, *24*, 6250–6259.
[20] U. Fekl, K. I. Goldberg, *J. Am. Chem. Soc.* **2002**, *124*, 6804–6805.
[21] S. M. Kloek, K. I. Goldberg, *J. Am. Chem. Soc.* **2007**, *129*, 3460–3461.
[22] M. W. Holtcamp, L. M. Henling, M. W. Day, J. A. Labinger, J. E. Bercaw, *Inorg. Chim. Acta* **1998**, *270*, 467–478.
[23] J. S. Yu, P. E. Fanwick, I. P. Rothwell, *J. Am. Chem. Soc.* **1990**, *112*, 8171–8172.
[24] M. Prinz, M. Grosche, E. Herdtweck, W. A. Herrmann, *Organometallics* **2000**, *19*, 1692–1694.
[25] Y. O. Ma, R. G. Bergman, *Organometallics* **1994**, *13*, 2548–2550.
[26] A. R. Dick, M. S. Sanford, *Tetrahedron* **2006**, *62*, 2439–2463.
[27] J. A. Johnson, D. Sames, *J. Am. Chem. Soc.* **2000**, *122*, 6321–6322.
[28] T. M. Douglas, J. L. Notre, S. K. Brayshaw, C. G. Frost, A. S. Weller, *Chem. Commun.* **2006**, 3408–3410.
[29] T. M. Douglas, E. Molinos, S. K. Brayshaw, A. S. Weller, *Organometallics* **2007**, *26*, 463–465.
[30] M. Grellier, L. Vendier, S. Sabo-Etienne, *Angew. Chem.* **2007**, *119*, 2667–2669; *Angew. Chem. Int. Ed.* **2007**, *46*, 2613–2615.
[31] R. Shintani, W.-L. Duan, T. Nagano, A. Okada, T. Hayashi, *Angew. Chem.* **2005**, *117*, 4687–4690; *Angew. Chem. Int. Ed.* **2005**, *44*, 4611–4614.
[32] C. Defieber, M. A. Ariger, P. Moriel, E. M. Carreira, *Angew. Chem.* **2007**, *119*, 3200–3204; *Angew. Chem. Int. Ed.* **2007**, *46*, 3139–3143.
[33] T. M. Miller, G. M. Whitesides, *Organometallics* **1986**, *5*, 1473–1480.
[34] R. L. Brainard, T. M. Miller, G. M. Whitesides, *Organometallics* **1986**, *5*, 1481–1490.
[35] S. Boulmaaz, M. Mlakar, S. Loss, H. Schönberg, S. Deblon, M. Wörle, R. Nesper, H. Grützmacher, *Chem. Commun.* **1998**, 2623–2624.
[36] H. Schönberg, S. Boulmaaz, M. Wörle, L. Liesum, A. Schweiger, H. Grützmacher, *Angew. Chem.* **1998**, *110*, 1492–1494; *Angew. Chem. Int. Ed.* **1998**, *37*, 1423–1426.
[37] S. Deblon, H. Rüegger, H. Schönberg, S. Loss, V. Gramlich, H. Grützmacher, *New J. Chem.* **2001**, *25*, 83–92.
[38] F. Breher, H. Rüegger, M. Mlakar, M. Rudolph, S. Deblon, H. Schönberg, S. Boulmaaz, J. Thomaier, H. Grützmacher, *Chem. Eur. J.* **2004**, *10*, 641–653.
[39] C. Laporte, F. Breher, J. Geier, J. Harmer, A. Schweiger, H. Grützmacher, *Angew. Chem.* **2004**, *116*, 2621–2624; *Angew. Chem. Int. Ed.* **2004**, *43*, 2567–2570.
[40] P. Maire, S. Deblon, F. Breher, J. Geier, C. Böhler, H. Rüegger, H. Schönberg, H. Grützmacher, *Chem. Eur. J.* **2004**, *10*, 4198–4205.
[41] G. Mora, S. van Zutphen, C. Thoumazet, X. F. Le Goff, L. Ricard, H. Grutzmacher, P. Le Floch, *Organometallics* **2006**, *25*, 5528–5532.
[42] P. S. Pregosin, R. W. Kunz, *^{31}P and ^{13}C NMR of transition metal phosphine complexes*, Springer, Berlin, **1979**.
[43] M. Ogasawara, S. A. Macgregor, W. E. Streib, K. Folting, O. Eisenstein, K. G. Caulton, *J. Am. Chem. Soc.* **1995**, *117*, 8869–8870.
[44] R. Abbel, K. Abdur-Rashid, M. Faatz, A. Hadzovic, A. J. Lough, R. H. Morris, *J. Am. Chem. Soc.* **2005**, *127*, 1870–1882.
[45] C. Böhler, N. Avarvari, H. Schonberg, M. Worle, H. Ruegger, H. Grützmacher, *Helv. Chim. Acta* **2001**, *84*, 3127–3147.
[46] M. J. Ingleson, S. K. Brayshaw, M. F. Mahon, G. D. Ruggiero, A. S. Weller, *Inorg. Chem.* **2005**, *44*, 3162–3171.
[47] K. Abdur-Rashid, D. G. Gusev, A. J. Lough, R. H. Morris, *Organometallics* **2000**, *19*, 1652–1660.
[48] M. Grellier, L. Vendier, B. Chaudret, A. Albinati, S. Rizzato, S. Mason, S. Sabo-Etienne, *J. Am. Chem. Soc.* **2005**, *127*, 17592–17593.
[49] D. Giunta, M. Hölscher, C. W. Lehmann, R. Mynott, C. Wirtz, W. Leitner, *Adv. Synth. Catal.* **2003**, *345*, 1139–1145.

[50] S. Li, M. B. Hall, J. Eckert, C. M. Jensen, A. Albinati, *J. Am. Chem. Soc.* **2000**, *122*, 2903–2910.
[51] M. Guizado-Rodriguez, A. Flores-Parra, S. A. Sanchez-Ruiz, R. Tapia-Benavides, R. Contreras, V. I. Bakhmutov, *Inorg. Chem.* **2001**, *40*, 3243–3246.
[52] T. Gottschalk-Gaudig, J. C. Huffman, K. G. Caulton, H. Gerard, O. Eisenstein, *J. Am. Chem. Soc.* **1999**, *121*, 3242–3243.
[53] T. Aoki, R. H. Crabtree, *Organometallics* **1993**, *12*, 294–298.
[54] W. W. Xu, G. P. Rosini, M. Gupta, C. M. Jensen, W. C. Kaska, K. Krogh-Jespersen, A. S. Goldman, *Chem. Commun.* **1997**, 2273–2274.
[55] F. L. Taw, H. Mellows, P. S. White, F. J. Hollander, R. G. Bergman, M. Brookhart, D. M. Heinekey, *J. Am. Chem. Soc.* **2002**, *124*, 5100–5108.
[56] W. J. Oldham, A. S. Hinkle, D. M. Heinekey, *J. Am. Chem. Soc.* **1997**, *119*, 11028–11036.
[57] U. E. Bucher, T. Lengweiler, D. Nanz, W. von Philipsborn, L. M. Venanzi, *Angew. Chem.* **1990**, *102*, 573–575; *Angew. Chem. Int. Ed. Engl.* **1990**, *29*, 548–549.
[58] V. I. Bakhmutov, C. Bianchini, M. Peruzzini, F. Vizza, E. V. Vorontsov, *Inorg. Chem.* **2000**, *39*, 1655–1660.
[59] R. Gelabert, M. Moreno, J. M. Lluch, A. Lledos, V. Pons, D. M. Heinekey, *J. Am. Chem. Soc.* **2004**, *126*, 8813–8822.
[60] R. H. Crabtree, D. G. Hamilton, *J. Am. Chem. Soc.* **1986**, *108*, 3124–3125.
[61] M. H. G. Prechtl, Y. Ben-David, D. Giunta, S. Busch, Y. Taniguchi, W. Wisniewski, H. Goerls, R. J. Mynott, N. Theyssen, D. Milstein, W. Leitner, *Chem. Eur. J.* **2007**, *13*, 1539–1546.
[62] A. C. Cooper, O. Eisenstein, K. G. Caulton, *New J. Chem.* **1998**, *22*, 307–309.
[63] S. A. Macgregor, T. Wondimagegn, *Organometallics* **2007**, *26*, 1143–1149.
[64] S. M. Kloek, K. I. Goldberg, *J. Am. Chem. Soc.* **2007**, *129*, 3460–3461, and references therein.
[65] R. R. Schrock, J. A. Osborn, *J. Am. Chem. Soc.* **1971**, *93*, 2397–2407.
[66] Gaussian 03, Revision C.02, M. J. Frisch, G. W. Trucks, H. B. Schlegel, G. E. Scuseria, M. A. Robb, J. R. Cheeseman, J. A. Montgomery, Jr., T. Vreven, K. N. Kudin, J. C. Burant, J. M. Millam, S. S. Iyengar, J. Tomasi, V. Barone, B. Mennucci, M. Cossi, G. Scalmani, N. Rega, G. A. Petersson, H. Nakatsuji, M. Hada, M. Ehara, K. Toyota, R. Fukuda, J. Hasegawa, M. Ishida, T. Nakajima, Y. Honda, O. Kitao, H. Nakai, M. Klene, X. Li, J. E. Knox, H. P. Hratchian, J. B. Cross, V. Bakken, C. Adamo, J. Jaramillo, R. Gomperts, R. E. Stratmann, O. Yazyev, A. J. Austin, R. Cammi, C. Pomelli, J. W. Ochterski, P. Y. Ayala, K. Morokuma, G. A. Voth, P. Salvador, J. J. Dannenberg, V. G. Zakrzewski, S. Dapprich, A. D. Daniels, M. C. Strain, O. Farkas, D. K. Malick, A. D. Rabuck, K. Raghavachari, J. B. Foresman, J. V. Ortiz, Q. Cui, A. G. Baboul, S. Clifford, J. Cioslowski, B. B. Stefanov, G. Liu, A. Liashenko, P. Piskorz, I. Komaromi, R. L. Martin, D. J. Fox, T. Keith, M. A. Al-Laham, C. Y. Peng, A. Nanayakkara, M. Challacombe, P. M. W. Gill, B. Johnson, W. Chen, M. W. Wong, C. Gonzalez, J. A. Pople, Gaussian, Inc., Wallingford CT, **2004**.
[67] D. Andrae, U. Haussermann, M. Dolg, H. Stoll, H. Preuss, *Theor. Chim. Acta* **1990**, *77*, 123–141.
[68] A. Hollwarth, M. Bohme, S. Dapprich, A. W. Ehlers, A. Gobbi, V. Jonas, K. F. Kohler, R. Stegmann, A. Veldkamp, G. Frenking, *Chem. Phys. Lett.* **1993**, *208*, 237–240.
[69] P. C. Harihara, J. A. Pople, *Theor. Chim. Acta* **1973**, *28*, 213–222.
[70] W. J. Hehre, R. Ditchfield, J. A. Pople, *J. Chem. Phys.* **1972**, *56*, 2257–2261.
[71] G. T. Velde, F. M. Bickelhaupt, E. J. Baerends, C. F. Guerra, S. J. A. Van Gisbergen, J. G. Snijders, T. Ziegler, *J. Comput. Chem.* **2001**, *22*, 931–967.
[72] C. F. Guerra, J. G. Snijders, G. te Velde, E. J. Baerends, *Theor. Chem. Acc.* **1998**, *99*, 391–403.
[73] G. M. Sheldrick in *SHELXL97—A program for crystal structure refinement*, **1997**.
[74] L. J. Farrugia, *J. Appl. Crystallogr.* **1999**, *32*, 837.
[75] R. H. Blessing, *Acta Crystallogr. A* **1995**, *51*, 33.

Received: June 22, 2007
Published online: November 8, 2007

